ALUMINIUM AND NICKEL-DOPED ZINC OXIDE THIN FILMS FABRICATED THROUGH THE AQUEOUS SPRAY-COATING METHOD AND EVALUATIONS OF THEIR PHOTOCATALYTIC ACTIVITIES

A THESIS SUBMITTED IN FULFILMENT OF THE REQUIREMENTS FOR THE DEGREE OF

MASTER OF SCIENCE IN CHEMISTRY (BY THESIS)

OF

THE UNIVERSITY OF NAMIBIA

BY

WILKA NAALOMBOLE TITUS

201703636

OCTOBER 2025

SUPERVISOR: DR. PHILIPUS HISHIMONE (UNIVERSITY OF NAMIBIA)

ABSTRACT

This work introduces the aqueous spray-coating method to address the challenges in the fabrication of thin films for photocatalytic applications. The aqueous spray-coating method has shown to be an effective method for the fabrication of undoped, aluminium (Al), and nickel (Ni)-doped Zinc Oxide (ZnO) thin films on quartz glass substrates with many advantages, such as simple instrumentation set-up, inexpensiveness, the ease of controlling the rate of deposition, and high yield. An aluminium (Al^{3+}) complex salt was synthesised in this study as a source of Al^{3+} ions in the prepared precursor solutions for fabricating Al-doped ZnO thin films. The synthesised complex was characterised using Fourier transform infrared (FTIR) spectroscopy. The various thin films were fabricated by depositing the prepared aqueous precursor solutions containing Zn^{2+} complexes alone as well as Zn^{2+} with varying mole percentages (2, 4, 8, and 16%) of Al^{3+} or Ni^{2+} complexes onto pre-heated quartz glass substrates, and the as-sprayed films were heat-treated at 450^{o}C for 30 minutes. The structural, optical, morphological, and photocatalytic characteristics of the fabricated thin films were evaluated using X-ray diffractometer (XRD), ultraviolet–visible (UV–Vis) spectrophotometer and scanning electron microscope (SEM). The XRD results revealed that the fabricated thin films have a hexagonal wurtzite phase. The optical properties (absorbance and transmittance) of the fabricated thin films were analysed using the UV–Vis spectrophotometer, and all the fabricated thin films showed high transmittance in the visible region over 70%, even after Al and Ni doping. Experiments on methyl orange dye degradation in the presence of the fabricated thin films under visible light showed that Al-doped ZnO exhibits good photocatalytic activities that increase with an increase in the doping mole% of Al. On the contrary, Ni-doped ZnO thin films exhibited a very slight to no degradation of the methyl orange dye under the

same conditions. The highest degradation efficiency was obtained for 8% Al-doped ZnO thin films under visible light irradiation.

Keywords: Aqueous spray-coating method, thin films, ZnO, precursor solutions, hexagonal wurtzite phase, photocatalytic activity

LIST OF PUBLICATION(S)/CONFERENCE(S) PROCEEDINGS

Conference(s):

1. **W.N. Titus**, P.N. Hishimone. Investigations on the fabrication of Al and Ni-doped ZnO thin films by the aqueous spray-coating method and their applications as photoanodes for hydrogen production via photoelectrochemical water splitting. National Science Week Conference (6th – 10th November 2023), University of Namibia. Windhoek, Namibia.

2. **W.N. Titus**, P.N. Hishimone. Photocatalytic activities of aluminium-doped zinc oxide thin films fabricated via the aqueous spray-coating method. Chem4Energy Annual Conference – Materials and Processes for a Sustainable Energy Future (7^{th} – 11^{th} April 2025), Protea Hotel Walvis Bay Pelican. Walvis Bay, Namibia.

Publication(s):

W.N. Titus, A. Uusiku & P.N. Hishimone. (2025). Aluminium-doped zinc oxide thin films fabricated by the aqueous spray method, and their photocatalytic activities. Published in MDPI Journals.

Table of Contents

LIST OF TABLES

LIST OF FIGURES

LIST OF ABBREVIATIONS AND/OR ACRONYMS

Al	Aluminium
ALE	Atomic Layer Epitaxy
AZO	Aluminium doped ZnO
CB	Conduction Band
CVD	Chemical Vapour Deposition
DC	Direct Current
EDX	Energy Dispersive X-ray
FTO	Fluorine doped Tin Oxide
FCC	Face-centered cubic
FTIR	Fourier transform infrared
H_2	Hydrogen
LED	Light emitting diode
KBr	Potassium bromide
MBE	Molecular beam epitaxy
MO	Methyl orange
MOCVD	Metal-organic chemical vapour deposition
Ni	Nickel
PLD	Pulsed laser deposition
PEC	Photoelectrochemical

RF	Radio frequency
SEM	Scanning electron microscope
STH	Solar to hydrogen
SnO_2	Tin dioxide
TiO_2	Titanium dioxide
TCO	Transparent conductive oxides
UV-Vis	Ultraviolet-visible
VB	Valence band
XRD	X-ray diffractometer
ZnO	Zinc Oxide

UNITS AND MATHEMATICAL SYMBOLS

Å	Armstrong
°C	degree Celsius
µm	micrometres
g	grams
E.g	for example
eV	electron volts
ε	Molar absorption coefficient
hr/h	hour

L, L^{-1}	Litre, per litre
M, M^{-1}	Molar, per molar
mL	millilitres
mol, mmol	mole, millimole
mm^2, mm^3	square, cubic millimetres
cm, nm	centimetre, nanometre
ppm	parts per million
%, **%D**	Percentage, percentage degradation
θ	Theta
TW, **W**	Terawatts, watts

ACKNOWLEDGMENTS

I would like to thank God for giving me the ability and perseverance to complete this study and for his guidance and protection.

I would like to express my sincere gratitude to my supervisor, Dr. Philipus Hishimone, for his supervision, guidance, and willingness to help. It has been an honor to work with him, and I am forever appreciative of his insightful advice and the invaluable time he dedicated to reviewing my work.

I am thankful to the Department of Physics, Chemistry, and Material Science at the University of Namibia for providing me with all the research materials and facilities and the opportunity to pursue this degree.

My vote of thanks also goes to Hof University of Applied Sciences for hosting me to conduct a part of my research as a guest researcher and for providing me with all the necessary research materials and facilities.

My sincere gratitude goes to the Federal Republic of Germany and the government of the Republic of Namibia, in partnership with the Southern African Science Service Centre for Climate Change and Adaptive Land Management (SASSCAL), for fully funding this project.

I would like to thank my laboratory mates for their cooperation during laboratory work; their willingness to share valuable knowledge and engage in productive discussions has greatly contributed to the success of this research.

I am truly grateful to my family for their understanding, assistance, and encouragement throughout my study. Their support, emotional, physical, and financial, has been instrumental in helping me navigate the challenges of this academic journey.

DEDICATION

This thesis is dedicated to my parents, Helvi Mumati and Barkias Titus.

DECLARATIONS

I, **Wilka Naalombole Titus**, hereby declare that this study is my own work and is a true reflection of my research, and that this work, or any part thereof, has not been submitted for a degree at any other institution. No part of this thesis may be reproduced, stored in any retrieval system, or transmitted in any form or by means (e.g., electronic, mechanical, photocopying, recording, or otherwise) without the prior permission of the author or the University of Namibia in that behalf. I, **Wilka Naalombole Titus**, grant the University of Namibia the right to reproduce this thesis in whole or in part, in any manner or format, which the University of Namibia may deem fit.

Wilka N Titus		October 2025
Name of Student	Signature	Date

CHAPTER 1: INTRODUCTION

1.1. Background of the study

The prosperity of the world economy due to the rapid development of industrialisation has brought about severe energy and environmental issues, for instance, water pollution, soil contamination, and the greenhouse effect [1]. It is of no doubt that continuous utilisation of fossil fuels will worsen these problems [1]. Presently, humans are putting efforts into coming up with creative ways to produce energy that is affordable and is constantly replenished in order to tackle and lessen the effects of greenhouse gases [2]. The main obstacle to implementing a sustainable energy economy is the intermittent, random, and volatile nature of renewable energy sources like sunlight, wind, and water [3]. To close the gap between energy supply and demand, electricity can be stored, for example, in solar batteries or chemical bonds to power society when there are no renewable resources available [4].

Harnessing sunlight to produce clean fuels like hydrogen (H_2) is a desirable and sustainable approach toward meeting future energy demands without environmental impact [5]. About 100,000 terawatts (TW) of solar energy strike our globe annually, with an estimated 36,000 TW of that amount hitting the land, making solar energy the cleanest, ample, and renewable energy source on earth. [6]. However, the cost and efficiency of technologies that can be used have prevented solar energy from being developed into a practical technology for large-scale solar energy harvesting and reservation [7]. The use of photoelectrochemical (PEC) water splitting offers the potential to produce hydrogen from the sunlight with no incurring additional costs for the installation of a photovoltaic setup or the accompanying failure of such systems [8].

Photoelectrochemical (PEC) water splitting and water-splitting electrocatalytic reactions are two different concepts, with the latter being initiated and driven by electric current [9]. Nowadays, the primary method for producing hydrogen (H_2) is steam reforming of fossil fuels, but this approach gives off greenhouse gases as final products [10]. Therefore, using this technique to continuously produce H_2 will only present more environmental problems [10]. The combustion of green hydrogen produces solely water and a large amount of energy, making it a clean fuel that does not pollute the environment, and this positions it as a promising alternative energy source with the potential to address both environmental concerns and energy shortages [10]. For this plan to work, PEC water-splitting devices that are affordable, stable, efficient, and scalable are required for economically competitive hydrogen production on a global energy demand scale [11].

The outcome of a PEC water splitting system is highly influenced by the photocathode and photoanode materials used; hence, it is important to choose photoelectrode materials with optimal properties for the desired results [12]. The best photoelectrode materials must be made of earthly abundant semiconductors to make the process sustainable on a large scale, and their band gap should allow them to absorb sunlight and drive the water splitting reaction [12]. An approach to boost productive electron-hole detachment and movement can be used to avoid rapid charge recombination leading to minor solar to hydrogen (STH) conversions. The faster the photocatalytic activities are taking place, the fewer charges gather on the surface of the photocatalyst, and this leads to less chance of electron-hole recombination [12, 13].

Tin dioxide (SnO_2), cuprous oxide (Cu_2O), iron (III) oxide (Fe_2O_3), titanium dioxide (TiO_2), and zinc oxide (ZnO) have been used as semiconductor photocatalysts [14].

Out of these different semiconductors, ZnO has gained a lot of focus owing to the harmlessness, affordability, great electrical properties, and availability of zinc metal [2]. Moreover, ZnO has been largely investigated as a photoanode material because of its outstanding electron mobility and thermal and chemical stability; however, ZnO has a large band, and this narrows down its uses to the UV region of the electromagnetic spectrum [15]. A band gap energy corresponds to the photon energy required to excite an electron from the conduction band to the valence band of a semiconductor [15]. The band gap energy of ZnO (~3.37 eV) means that it can only be activated by photons with a minimum energy of 3.37 eV, and this energy corresponds to the UV energy. The integration of metal dopants into undoped ZnO thin films is considered an effective method to broaden their absorption window from ultraviolet to visible regions [16, 17].

The two dopants, aluminium and nickel, used in this study were chosen based on past literature [2, 18, 19], where they have been used as dopants for the fabrication of ZnO photocatalysts; however, the fabrication methods used were complicated, not environmentally friendly and expensive. This study will advance the fabrication method of ZnO thin films for application in photocatalysis. Besides that, aluminium and nickel are metal dopants that are said to behave as traps for the photogenerated charges and enhance the photocatalytic efficiency by obstructing the recombination rate of the charge carrier [20]. The abundance, low mass, and the ionic radius of Al^{3+} (0.54 Å), which is closer to that of Zn^{2+} (0.74 Å), make it a good dopant for ZnO [21]. On the other hand it is anticipated that Ni^{2+} can substitute Zn^{2+} without altering the crystal structure of ZnO, because they have similar valence electrons and their ionic radii are close [22].

Sun light gets to the earth's surface largely in the infrared and visible regions, with ultraviolet light accounting only for a minor five percent, and this highlights the requirement for studies to create materials that can also be activated by visible light [23]. Although huge attempts have been compiled in the last ten years to attain the desired characteristics in semiconductor materials that at the same time fulfil the affordability, high productivity, and steadiness requirements for PEC water splitting systems. Research is still ongoing in search of new materials and the improvement of existing low-cost photoelectrode materials [24]. Hence, this research explored the fabrication of Al and Ni-doped ZnO thin films by the aqueous spray-coating method and evaluation of their photocatalytic activities for various photocatalytic applications.

1.2. Statement of the problem

The process of photocatalysis utilises photocatalysts (e.g. photoanodes and photocathodes) to absorb light and allow the redox reactions to take place. The existing photocatalysts are either ineffective or fabricated through unsustainable methods. There have been efforts to develop various photocatalysts that can drive the photocatalytic reaction by direct use of sunlight. However, the fabrication of such materials is not simple; hence, there is a need for a simple yet effective fabrication method for photocatalytic materials. The aqueous spray-coating method presents a simple, cost-effective, and scalable approach to fabricating these materials, but its effectiveness in producing high-performance photocatalytic materials has not been explored thoroughly.

1.3. Objectives of the study

The main purpose of this study was to use the aqueous spray-coating method to fabricate ZnO thin films doped with Al and Ni and evaluate their photocatalytic activities.

The specific objectives of this study were to:

a) prepare the precursor solutions containing Zn^{2+} complexes only, as well as Zn^{2+} and Al^{3+} / Ni^{2+} complexes
b) fabricate undoped, Al, and Ni-doped ZnO thin films using the prepared precursor solutions
c) characterise the structural, optical, and morphological properties of the fabricated thin films by XRD, UV-Vis spectrophotometer, and SEM
d) evaluate the photocatalytic activities of the fabricated thin films.

1.4. Significance of the study

This study led to the development of a facile method for Al and Ni-doped ZnO thin films fabrication, which is the aqueous spray-coating method. It revealed the effects of various dopants on the properties of thin films, which significantly contributes to the fabrication of photocatalytic materials that are efficient, stable, effective, and scalable.

1.5. Delimitations of the study

The delimitation of the study was that the research was limited to focus only on the fabrication of Al and Ni-doped ZnO thin films by the aqueous spray-coating method and evaluate their photocatalytic activities.

CHAPTER 2: LITERATURE REVIEW

2.1. Thin films

A thin film is a material measuring less than one micrometre (μm) in thickness, that is fabricated on a supporting substrate by amplifying one-by-one ionic, molecular, or atomic species of matter [25]. The evolution of research on thin films started about a hundred years ago; however, they have only been used recently at a large extent in feasible settings [26]. The increase in the number of studies on thin films is attributed to their uses in the different areas of defence, optics, electronics, space science, and other industries [26]. The properties of thin films can be customised, and this has led to their utilisation in different areas, from modern applications such as antireflective coatings and photovoltaic devices to coatings for corrosion and scratch protection [27].

The common daily uses of thin films are the household or vehicle mirrors, which normally have a coloured coating on the back of a glass sheet to form a reflecting border [28] and the mobile and computer touch panel, which uses a transparent conductive thin film and an anti-reflection thin film on the glass [29]. When it comes to the uses, characteristics, and financial aspects, thin films have a lot of benefits over their massive equivalence [30]. Some of these benefits are that fabricating thin films replaces expensive and in-short-supply materials because of their low cost, and they have great function because of the much improved ionic and electronic conductivity, increased surface area, and the ease of controlling their sizes and shapes [31].

As a result, the electronic sectors are focusing on producing devices that are lighter, smaller, and have a low consumption of energy [32]. For instance, thin film lithium-ion batteries are composed of thick materials with micrometres or nanometres measurements, allowing for a finished battery of just millimetres in thickness. They give the same power as the bigger batteries but have thinner proportions [26]. Materials can be easily converted into a range of devices by being fabricated as thin films; hence, the majority of functional materials are rather implemented in thin film form owing to their unique structural, optical, and electrical properties [28]. When designing heterojunctions with n-type oxide thin films for the fabrication of thin film devices, transparent metal oxide thin films of p-type semiconductors deposited directly on different substrates provide a number of benefits [29].

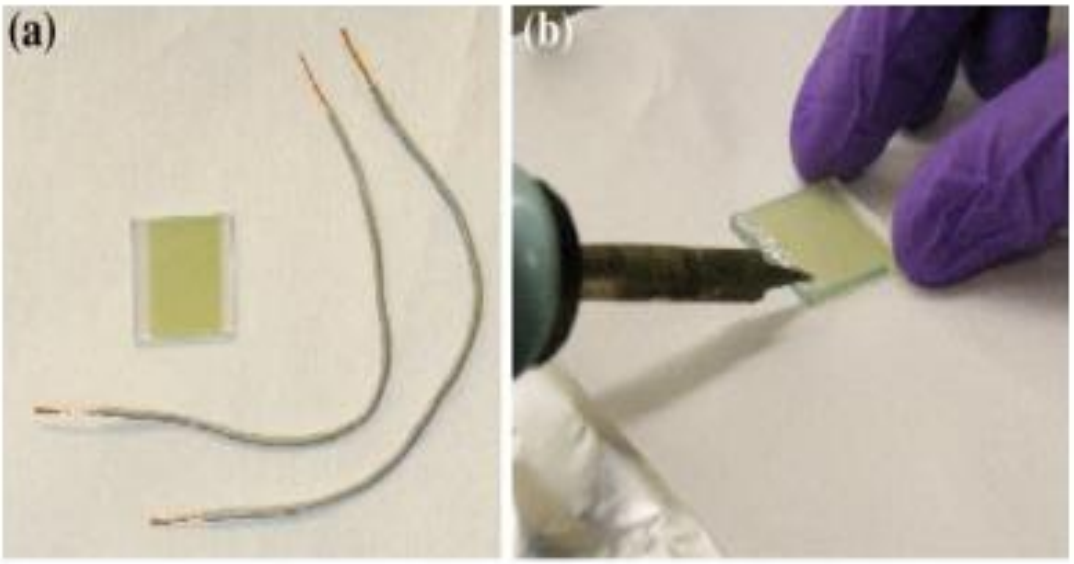

Figure 1. Images of thin films on a supporting substrate with a masking [33]

2.2. Zinc Oxide

Zinc oxide, which has the chemical formula ZnO, is an inorganic substance that is insoluble in water and usually appears as white powder [34]. It is found as the mineral

zincite in the Earth's crust; however, it is worth mentioning that most wholesale ZnO used is man-made [35]. Cubic sphalerite, hexagonal wurtzite, and cubic rock salt are the phases of ZnO, and at room temperature, the hexagonal wurtzite phase is the most constant one [36]. The qualities of ZnO, such as high electron mobility and thermal conductivity, a wide bandgap, being highly abundant, and being non-toxic, make it a valuable material [37]. ZnO as an additive is popularly utilised in by-products and substances, including cosmetics, ceramics, glass, electronics, and even pharmaceuticals [38].

The use of ZnO in the present day is calamine lotion in the form of a slurry of zinc and iron oxide [39] and in sunscreen components as a physical barrier against UV radiation [40]. The wide range of applications of ZnO has led to its investigation in various forms, for instance, thin film and powder forms [21]. Thin films of ZnO have been reported to have promising uses in transparent conductive oxide (TCO) devices, UV photodetectors, solar cells, photocatalysts, gas sensors, or biosensors owing to their optical (photoluminescence), electrical (thermoelectric, piezoelectric), and biological (antibacterial) properties [41]. In spite of the potential uses of ZnO in different areas, the effectiveness of ZnO is restricted by its high resistivity, large bandgap, and inadequate charge transfer [42]. New approaches for adjusting ZnO's characteristics, that is, coupling with other semiconductors and doping with metal or nonmetal ions, have been made possible by the developing nanotechnology, which will extend its utilisation [42].

2.3. Doping zinc oxide thin films

Doping can be defined as an intentional addition of materials (dopants) into another material during the manufacturing process with the purpose of inducing specific alterations in its characteristics [43]. The dopant used in the process of doping should

be capable of either accepting or adding electrons, which will result in changes of the electrical features of the starting material [44]. Doping has a high likelihood of altering the band gap, photo response, oxygen vacancy creation, structural, morphology, surface area, and energy level of materials [45]. The enhancement of the ZnO band gap consequently promotes its efficiency in photocatalysis [46]. Two types of metal doping have been reported, namely substitutional doping and interstitial doping [47, 48].

Substitutional or replacement doping is the process of substituting the host atom when impurity atoms are positioned at regular lattice positions. For substitutional doping to occur, the solubility, atomic radii, crystal structure, and the electronegativity similarity between the dopant and main material must be fulfilled [47, 48]. Contrarily, the presence of impurity atoms between normal lattice sites, as shown in the figure below, is regarded as interstitial doping. A bigger variation amid the atomic radii of the dopant and the host material leads to the dopant locating in an interstitial area; this is the easiest way to predict the type of doping [47].

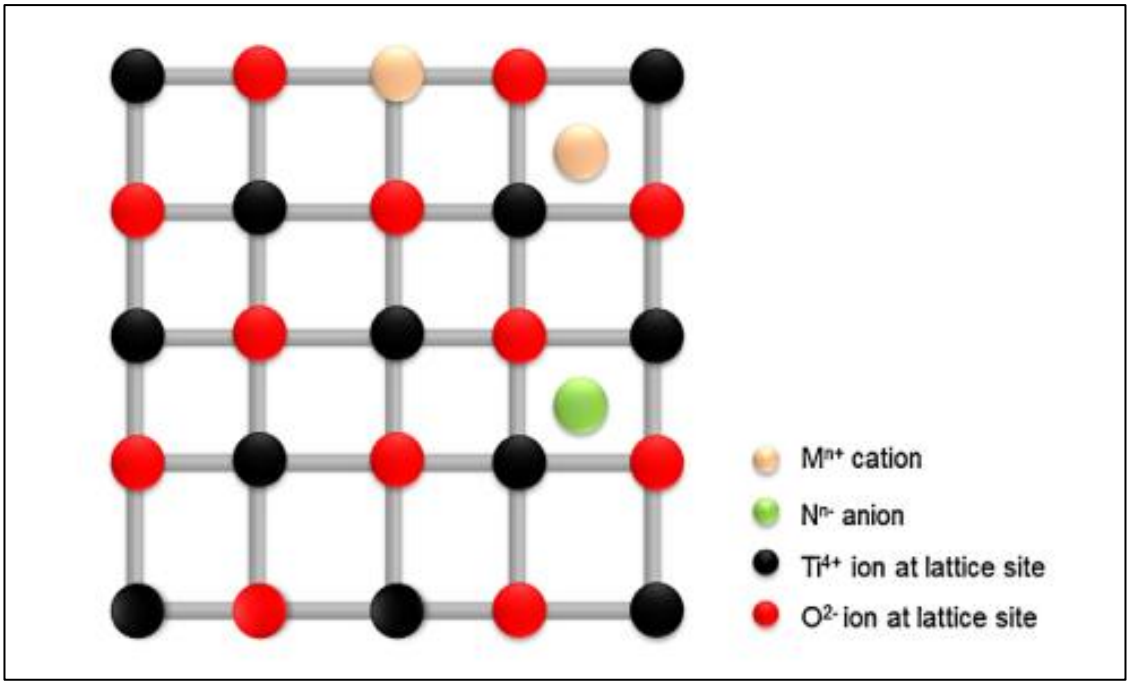

Figure 2. Illustration of the two types of metal doping, substitutional and interstitial are shown in the crystal lattice of TiO_2 [47]

When added to ZnO, elements from groups II, III, rare earth, and transition metal ions such as Mg, Al, Ce, La, Ni, Cr, Cu, and Co improved its optical, electrical, and structural characteristics [49–52]. Thin films of ZnO exhibit intriguing structural, morphological, and photoresponse properties upon doping with metal elements such as aluminium [21], chromium [15, 53], and nickel [2, 54]. The abundance, low mass, and the ionic radius of Al^{3+} (0.54 Å), which is closer to that of Zn^{2+} (0.74 Å), make it a good dopant for ZnO. The doping of ZnO thin films with aluminium was reported to exhibit a rise in transparency and the bandgap of thin films [21]. With the incorporation of nickel in ZnO, an increase in the absorbance and low resistivity were observed [54]. Without altering the crystal structure of ZnO, it is anticipated that Ni^{2+} can substitute Zn^{2+} because they have similar valence electrons and their ionic radii are close [22]**.** Even though these were some of the results for these dopants, two thin

films fabricated by different techniques with the same precursor materials will have various properties; hence, the fabrication method is of great importance [55].

2.4. Established methods for the fabrication of thin films

Apart from doping, the effective technological application of thin films requires considering the impact of the fabrication process on their qualities [56]. As a result, various methods, such as spin coating [57], dip coating [58], chemical vapour deposition (CVD), sol-gel [59], pulsed laser deposition (PLD), magnetron sputtering, spray pyrolysis [60], molecular beam epitaxy (MBE), and atomic layer deposition (ALD) [61], have been employed to fabricate thin films on different substrates. The liquid phase and the gas phase preparation methods are the two groups into which these techniques can be categorised.

The materials used in the gas phase processes are in the gaseous form; plain thin films are produced once they are altered physically or chemically, followed by cooling down. Photocatalysts with desirable properties can be fabricated by gas phase methods, but the downside of these techniques is that they use expensive and complicated instruments [62]. On the other hand, the liquid state techniques prepare thin films by mixing metal chemical salts in a solvent, mainly water or alcohol, followed by their precipitation and calcination to yield thin films or nanoparticles [62]. Some of the commonly used approaches are shown in the table below. Moreover, these techniques are fully discussed below, outlining their advantages and disadvantages.

Table 1. Some of the commonly used methods for the fabrication of thin films

Gas phase fabrication methods	Liquid phase fabrication methods
1. Chemical vapour deposition	1. Sol-gel
2. Magnetron sputtering	2. Spray-pyrolysis

3. Atomic layer deposition	3. Spin coating
4. Pulsed laser deposition	4. Dip-coating

2.4.1. Gas phase fabrication methods

Chemical Vapour Deposition technique

In the chemical vapour deposition method, the substrate to be coated and the chemical precursor are positioned at a pre-set distance in the reaction chamber [63]. The reaction chamber has a gas pipeline supply, normally argon gas, to direct the flow of the precursor to the substrate, and the chemical precursor utilised can be in a gas, liquid, or solid form. When the chemical precursors are either solid or liquid, they are first heated up to their evapouration point, and then they can be deposited on the substrates as a vapour. The CVD process can be operated in a closed or open chamber; however, the closed system is mostly used due to the benefits of safety, and fewer materials are utilised, whereas a constant supply of chemical precursors is required in an open system [64].

The CVD process has the benefit of adjustable deposition rates, being able to produce coatings of different layers that are well adhered to the substrate and require less manual work [65]. CVD allows the usage of a variety of chemical precursors, including hydrocarbons, metal organics, and metal halides. However, using precursor gases that are toxic, corrosive, flammable, and explosive can present inherent safety and chemical risks, and it can be challenging to deposit multicomponent materials. Additionally, it requires very high temperatures, a constant gas supply, more precursor

materials are used, and the process is time consuming, making it more expensive and unfeasible [65].

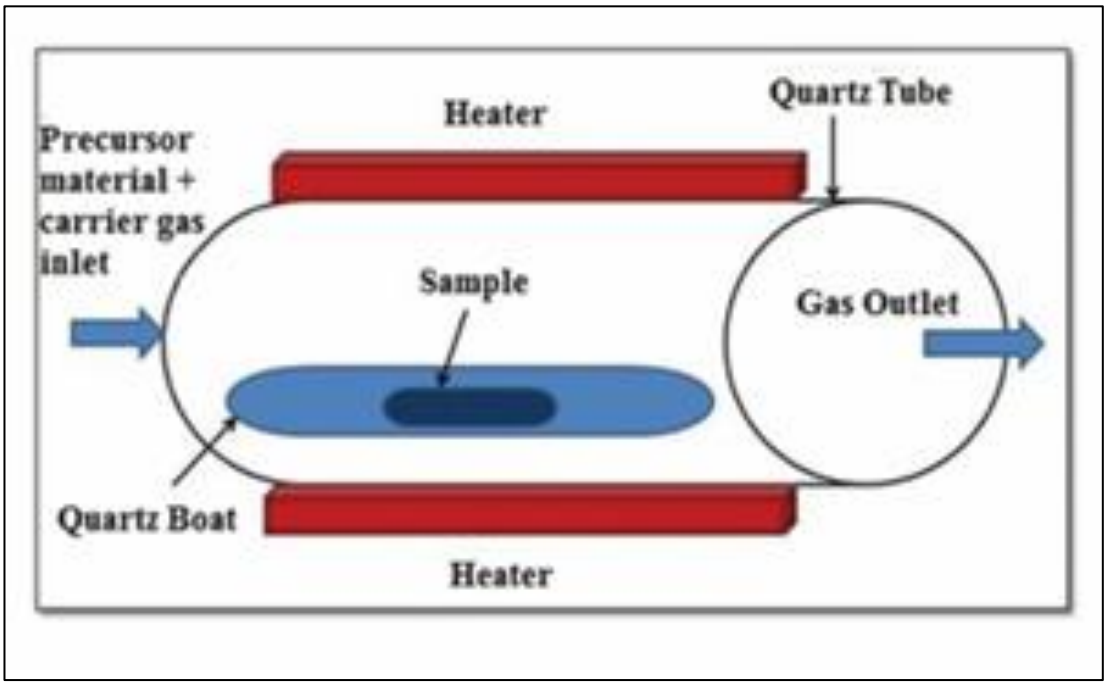

Figure 3. Diagram showing the different component of the chemical vapour deposition reactor [64].

Atomic layer deposition technique

Atomic layer deposition (ALD), also called atomic layer epitaxy (ALE), is a popular method that can deposit thin films layer by layer. This method was established and progressed in the fabrication of thin films of semiconductor substances at the commercial level [66]. The advantages of ALD deposition are the ability to deposit multiple layers, the ability to coat materials with complicated dimensions, and the low growth temperature. However, with this method, it is not easy to control the thickness, porosities, voids, and composition of the layer materials. This method is also not environmentally friendly as it could give off toxic byproducts [66]. The ALD process takes place in an ALD reactor, and the main components are the carrier gas, which can either be nitrogen or argon, a heater, a vacuum pump, and a thermocouple [67]. The

precursor material enters the reactor with the aid of the carrier gas and reacts with the substrate for a specified amount of time; the extra precursor materials and the end products are removed with the carrier gas [67]. The opposite precursor is then blown in the reactor, followed by the removal of products and excess precursor materials. These procedures result in the formation of one layer, and by repeating these steps, more than one layer can be fabricated [66, 67].

Magnetron sputtering technique

The magnetron sputtering method initiates by placing a thin film supporting substrate in a vacuum chamber filled with an unreactive gas, argon. The voltage is applied between the chamber and the coating material opposite the substrate, with the purpose of turning the coating material into a cathode, which is negatively charged. The existing free electrons in the chamber experience an electric field and move away from the negatively charged cathode [68]. When these electrons encounter high energy collisions with neutral atoms in the chamber, their electrons are knocked off and they form cations. The process proceeds until there is a plasma that is positively charged and the cathode attracts the plasma, and since they travel at high velocity, the negative ions sputter off the cathode and travel to the target substrate, and this way a coating is formed [68].

The variables to consider in this process are incident angle, mass of the atom in the target, mass of ions, and energy of ions, and these ions are obtained from an ionised gas, which can be argon [69]. The advantages of this method are the control of the growth speed, the possibility to obtain ultrathin films, high efficiency, the ability to be utilised at an industry scale, as well as the potential to utilise various supporting substrates in this process [69]. Even though the magnetron sputtering method is well established and has the capacity to fabricate thin films with superior properties and of

similar form with the target materials, it is not straight forward, requires procedures with very high vacuum, and it is costly [31]. There are a variety of magnetron sputtering techniques classified as radio frequency (rf) and direct current (dc) magnetron, and they are differentiated by the energy source utilised. Although only electrically conductive targets like doped semiconductors or metals are applied in direct current magnetron sputtering, it is quite affordable in contrast to radio frequency magnetron sputtering [32].

Pulsed laser deposition technique

High-quality thin films of materials have been fabricated through the pulsed laser deposition (PLD) method, and for a material to be coated on the substrate, it is hit with great energy laser [70]. As illustrated in the image below, the melted, evaporated, and ionised material on the surface of a target comes from the target in the form of plasma to a suitably placed substrate where it accumulates and condenses, and the thin film grows onto the substrate [70]. The PLD method depends on the productive interactivity of a liquid or solid target with the ultraviolet laser radiation, arising in the removal of substances from the surface of the target and successive settling on a supporting substrate [71].

While optimising, this process can require more time and effort than other methods due to the many variables at play. The quality of thin films depends on factors like laser wavelength, gas pressure, pulse duration, and target distance [72]. On the other hand, the high deposition rate, the ability to transfer stoichiometry of the material from the target to the substrate, the ability to deposit multiple layers, and the flexibility in power density and wavelength are some of the benefits of the PLD method [71]. Additional merits of the PLD method are an unlimited degree of freedom in the ablation geometry, control of growth rate, and versatility [71]. Certain devices, such

as photodetectors, photovoltaic cells, superconductors, electro stimulators, and light emitting diodes, have been fabricated recently using the PLD method [71].

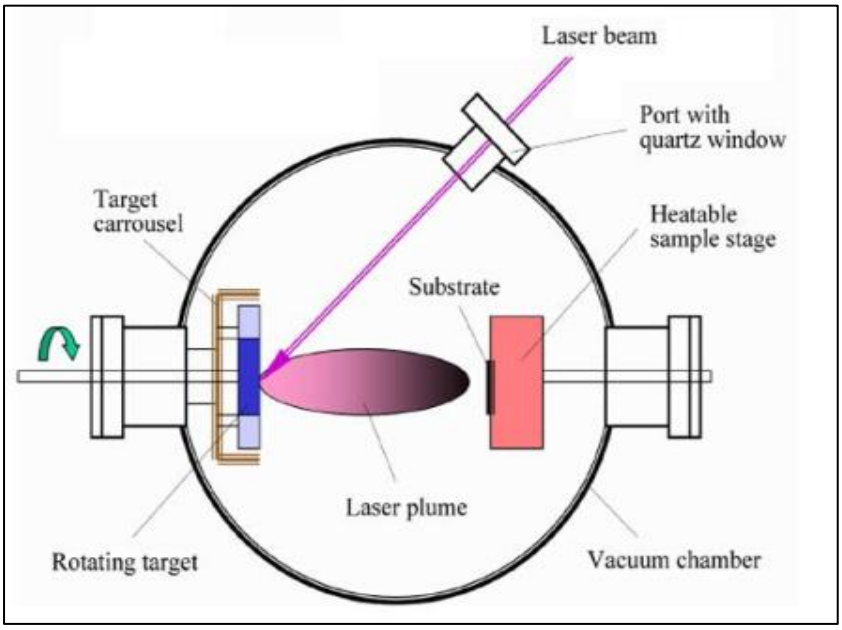

Figure 4. Pulsed laser deposition method setup [72]

2.4.2. Liquid phase fabrication methods

Sol-gel method

New materials have been fabricated in a convenient and cost-effective way utilising the Sol-gel method. The sol-gel method takes a straight forward approach to fabricate many components with the same set-up, allowing the growth of a well-linked network structure that is highly organised, and by mixing various precursor solutions, mixed oxides that are evenly distributed are made [73]. The benefits of the sol-gel technique are its ease of utilising, controllability, capacity to produce nano-sized particles with large surface areas in vast amounts and low cost [74]. Consequently, sol-gel is mostly applied in different sectors in contrast to other existing techniques because of these benefits [73].

[74]. Despite its advantages, the sol-gel technique has drawbacks such as long processing times, toxic organic solutions, contraction during processing, and residual hydroxyl or carbon groups [75]. In this method, the starting material is disintegrated in a solvent, usually alcohol or water, and through heating while stirring, a gel is formed by the process called alcoholysis or hydrolysis, depending on the solvent used. The gel obtained from the alcoholysis or hydrolysis process is not free of the solvent, and it should be dried in the correct way based on the required features and the gel used [76]. Following the drying step, the resultant gels are turned into nanoparticles and then heat-treated [76].

Spray pyrolysis method

The word pyrolysis originated from two words: pyro, which means heat, and lysis, meaning breaking. Thus, pyrolysis is the application of high temperature to disintegrate molecular compounds into basic elements [77]. There are several steps involved in spray pyrolysis, starting with the selection of the appropriate chemical reagents that are soluble in the solvent to be used and can be removed by calcination together with the unwanted products, and the solvent used should evaporate easily. This should happen at temperature of deposition, once they are sprayed onto the preheated substrate or at the post calcination step [77]. The supporting substrate is warmed up prior to spraying the well dissolved precursor solution consisting of respective elements of the preferred complex via a spray nozzle onto the substrate [72].

The sprayed-solution in a mist form should evaporate before touching the substrate or react with it post splashing, and the desired formation of a thin film with specific properties can be done at the optimum substrate temperature [72]. The spray pyrolysis method is applied for various applications owing to its cost-effectiveness, forging it to

be an economically feasible choice [78]. Additionally, the method is easy to put into effect, not complicated, has few steps, and effortless equipment assembly [78]. This technique's shortcoming lies in monitoring the solution flow, the gas pressure, and other variables like solute concentration and temperature, which can impact the final product [69].

The spin coating method

The spin coating approach is attractive for thin-film deposition because it can be scaled up easily, grows thin films at a reasonably low temperature, works well with flexible organic substrates, and is also inexpensive and less toxic. The primary drawback of this method is its low material efficiency, and the large substrates cannot be spun quick enough to enable the film to thin [79]. The four important steps in the spin coating in the fabrication process are spin-off, deposition, spin-up, and evaporation of solvent, as shown in the figure below. Firstly, the solution to spin coat is deposited in the middle of the substrate; when this is carried out if the substrate is rotating at a low speed, it is said to be a dynamic deposition or not rotating, referred to as static deposition [80].

The solution is then spread into a uniform thin film by rotating the substrate at a high speed, and at last, drying is done to detach the unused solvent, and a solid thin film is attained [81]. The rotating time of the spin coater and the spin speed directly influence the thickness of the resultant layer [80]. The third step (flow controlled) and fourth step (evaporation controlled) are the most vital since they have the biggest impacts on the thickness of the final coating. Besides the fourth step occurring during the whole preparation procedure, the first three steps are taking place consecutively [80]. Using such a simple and straight-forward procedure, a well-designed thin film can be produced [81].

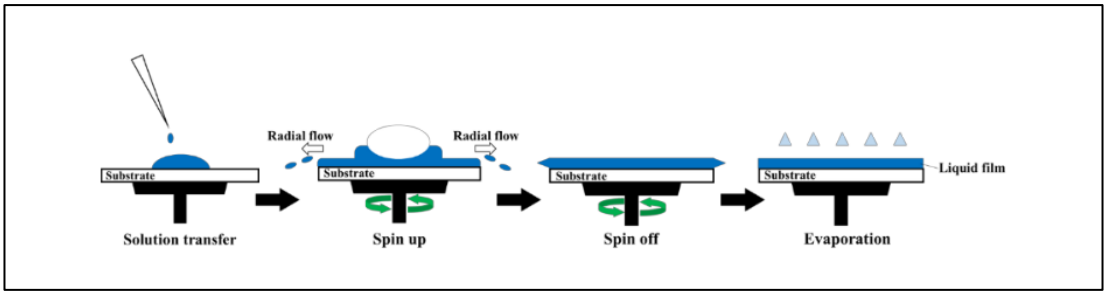

Figure 5. Schematic representation of the steps involved in the spin coating method [25]

The dip-coating method

The dip-coating technique is utilised in laboratories and industrial uses for thin film fabrication because it is facile, produces high-quality coating fast, and is of low cost. The method is mostly utilised for optical coatings, such as household mirror coating, antireflective coatings for sunglasses, vehicle rear view mirrors, and dye processing [82]. During the dip-coating process, the substrate is repeatedly immersed in the solution and taken out at a steady speed; a film of materials that do not evaporate is then attained on top of the drying curve. The suitable solvents used are normally alcohols because of their low adhesion to surfaces and their volatile nature to enhance rapid drying [58].

The dip-coating technique has the capacity of coating substrates with shapes that are not exposed or they are curved; however, there is a great amount of the precursor solution wasted through the process since the solution container utilised should contain adequate solution to cover the substrate upon dipping [82]. In the dip-coating method, the thickness of thin films can be regulated by the solution resistance to flow and the pace at which the substrates are removed from the solution. In spite of the coating solution having a long deposition time, huge solution containers that can hold a lot of coating solutions are required, and not all of the solution can be used [82]. The

appearance and width of the thin film in this method are influenced by density, substrate area, duration of immersion, surface tension, rate of removal, dip-coating cycles, coating solution evaporation rate, and solution resistance to flow [82].

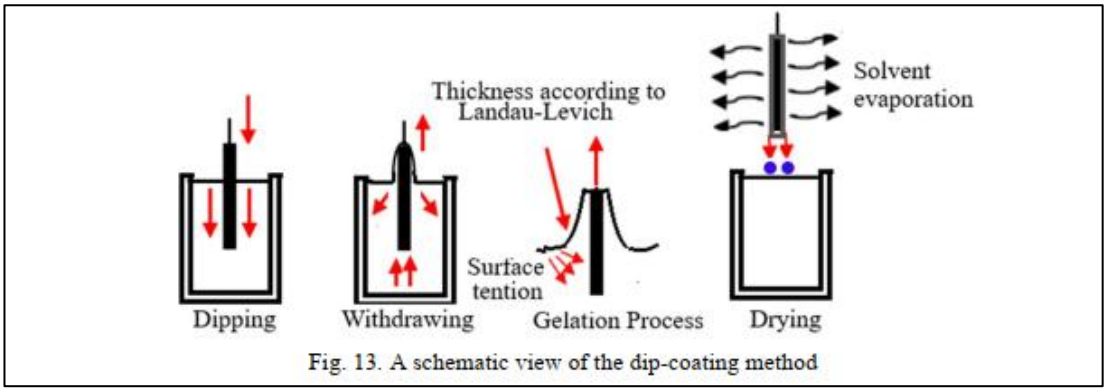

Fig. 13. A schematic view of the dip-coating method

Figure 6. Schematic view of the steps in the dip-coating method [72]

2.5. The aqueous spray-coating method

Although the above-mentioned methods are well established and able to fabricate superior quality thin films, they are associated with many complex negative attributes. The spray-coating method is an emerging and ideal method for this study because of its many advantages, including its low cost, simple instrumentation set-up, high yield, reduced material losses, ability to fabricate thin films reel to reel, and ability to be adjusted for large-area deposition [83]. The coatings can be easily patterned by shadow masking, and a wide range of precursor solutions with various rheologies, including aqueous solutions, can be utilised to attain any type of thin film, and by changing the amount of solution used, the thickness of the spray-coated layer can be regulated [84].

In spray-coating, an in-house-assembled system is used, which consists of a spraying nozzle with a solution contained and linked to a carrier gas source. The pressure of the carrier gas pulls the precursor solution through the nozzle, creating a mist of very small

droplets towards the pre-heated substrate. The substrate temperature is usually adjusted based on the used solvent because high solvent volatility is needed for the formation of the film [85]. Spray-coating relies on the formation of complexes of metal salts within the coating solutions, where thin films are attained after heat-treating sprayed films resulting from coating solutions onto thermally stable substrates [25]. All of these steps must be absolutely comprehended and regulated precisely to get standard spray-coated thin films with great properties [86].

During spray coating, multiple steps are involved; firstly, it involves the atomisation of a liquid solution or mixture into fine droplets. Subsequently, these droplets undergo flight and evaporation as they travel towards the substrate. Upon reaching the substrate, the droplets impact and spread, with phenomena such as spreading, receding, and recoiling influencing the coating's uniformity and thickness. The drying process follows, crucial for the solute adhesion and bonding to both itself and the substrate [86]. The successful fabrication of thin films using the spray-coating method has been extensively documented in academic and industrial research, with numerous studies reporting positive outcomes [25, 31, 83–88]. Looking at the abundance of varnishes and paints that come in spray devices, the spray coating process has shown to have a great potential in research on photoelectric devices for covering surfaces due to its low costs, its high material efficiency, and its suitability to simplify production [82]. All things considered; the above methods are being used to fabricate thin films for various purposes.

2.6. Zinc Oxide thin films as photocatalysts

Researchers have studied the photocatalytic potential of semiconductor materials like zinc oxide, magnesium oxide, iron oxide, and titanium dioxide for water refining uses [89]. Among these semiconductors, ZnO stands out as a powerful contender because of its distinctive qualities and superior photocatalytic performance as a photocatalyst [90]. ZnO is reported to have better quantum yield, strong oxidation properties, higher electron mobility, and high photostability under light irradiation in comparison to its competitive rival TiO_2 [89]. Studies reported that ZnO exhibits almost similar photocatalytic efficiency as TiO_2 in the degradation of various organic contaminants, but TiO_2 is more costly than ZnO, which makes ZnO effective in water treatment technology [91].

ZnO, having a direct bandgap and high electron mobility, excels in optoelectronics, specifically in light-emitting diodes and ultraviolet photodetectors, due to its strong exciton binding energy [89]. However, ZnO suffers from photocorrosion and dissolution in aqueous environments**,** limiting its long-term stability [91, 92]. In comparison, TiO_2, despite its larger bandgap and lower electron mobility**,** is mainly preferred for photoelectrochemical water splitting and photocatalysis due to its excellent resistance to photocorrosion and chemical stability [91]**.** Even though ZnO allows faster charge transfer, making it promising for high-efficiency photoelectrochemical applications, TiO_2 remains more dependable for long-term hydrogen production and environmental remediation [89, 91].

A large surface area of ZnO nanoparticles can promote higher adsorption of pollutant compounds on the particles surfaces, which are ultimately broken down into harmless products [89]. Although photocatalysts are normally utilised in powder form due to the associated large surface area, when they are used for environmental purposes, they

are preferred as thin films because this way they can be continuously used and it is easier to separate them from solutions in contrast to when photocatalytic nanoparticles are used [93]. An additional benefit of using ZnO thin films as photocatalysts, is that because they can be reused it makes the process fast and efficient [94].

According to literature, a pure ZnO thin film photocatalyst can be used for effective photocatalytic activities; however, the photo-excited electrons are unstable and they can move back to the valence band, resulting in low photocatalytic activities [95]. The quantum yield of the photocatalytic reaction is decreased by the recombination of electrons and holes in the valence band [18]. Doping ZnO with a metal enhances the photocatalytic efficiency by retarding the recombination rate of the charge carrier since metal dopants behave like traps for the photogenerated charges and that improves their average lifetime [20]. The captured charges then move to the surface of the thin film, where they break down the dye molecule, resulting in increased photocatalytic efficiency [18, 96]. The figure below illustrates the effect of doping where Al was used as a dopant.

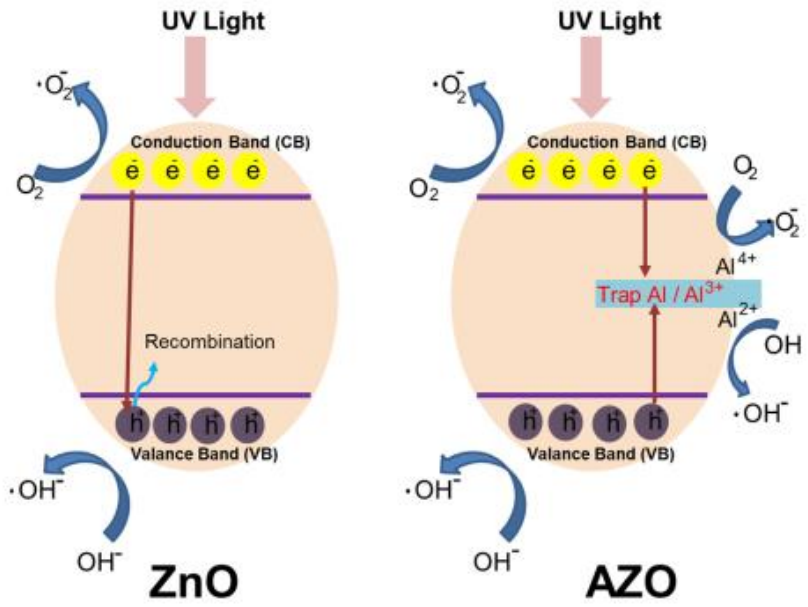

Figure 7. Diagrams showing the effect of Al doping into ZnO during photocatalytic process [18]

Although ZnO thin films are largely used in different applications, they experience challenges when it comes to stability under diverse environmental conditions. ZnO photocatalysts suffer from photocorrosion; under prolonged light exposure degradation of the material occurs, which restricts their practical utilisation in photocatalysis [91]. ZnO thin films were observed to be unstable in moist and aqueous conditions**,** resulting in gradual dissolution, and this can limit their long-term performance in water-based uses [92]. ZnO thin films also suffer from poor chemical stability in low pH**,** where lattice degradation and surface defects accelerate [92]. Thermal instability is another critical issue; at elevated temperatures ZnO undergoes structural changes, affecting its crystallinity and functional properties [97]. These limiting issues highlight the need for doping, the use of other fabrication techniques, or composite material integration to improve the dependability and durability of ZnO thin films for feasible utilisations [91].

2.7. The process of photocatalysis

By definition, photocatalysis is referred to as a reaction that uses light to start a photocatalytic material, which speeds up the chemical reaction pace without it being changed by the chemical reaction [95]. The effectiveness of the photocatalysis procedures rely on the light-absorbing ability of the photocatalysts [98]. The significant advantage of photocatalysis is its capacity to harness solar energy as an abundant, sustainable, clean, and renewable energy [98]. Recently, semiconductor-assisted photocatalysis is considered a good approach for cleaning up environmental pollution and for the creation of sustainable energy production. This approach aligns closely with the zero-waste discharge principle used in industrial effluent treatment, and it is valued for being affordable and environmentally friendly [48].

The process of photocatalysis can either be heterogeneous or homogeneous depending on the state of the photocatalyst used to that of the reagents. Homogeneous photocatalysis occurs when both the reactants and the photocatalyst are in an identical state, generally in a liquid or a gas state [99]. An example of a homogeneous photocatalytic reaction is when hydrogen peroxide is energised for the decomposition of tartaric acid in the company of iron [99]. The benefit of homogeneous photocatalysis is the high selectivity in breaking down pollutants, resulting in outstanding photocatalytic outcomes because of the even distribution. The drawbacks are that after the processes are concluded, such substances are difficult to set apart and their performance is restricted by working temperature [62].

On the other hand, when the photocatalyst is not in the same phase as the reactants, this is referred to as heterogeneous photocatalysis; for instance the application of a nanoparticle or solid catalysts in a liquid reaction mixture [99]. Heterogeneous photocatalysis has been broadly studied due to their uses in the fields of energy-related applications, improvement of environment, and organic synthesis [48]. The process takes place at room temperature, materials are completely degraded into harmless products, the oxygen needed for the reaction can be attained from the atmosphere, the catalyst is inexpensive, readily available, non-toxic, and can be recycled, the catalyst photo-excitation energy can be harnessed from the sun, all these features make the process appropriate to the remediation of contaminated water [100].

Photocatalytic process occurs when a semiconductor photocatalyst is irradiated with light and it absorbs the light energy equal to or greater than its band gap energy, the absorbed light excites the electrons from the valence band to the conduction band of the photocatalyst leaving behind holes in the valence band [101]. The holes in the valence band moves to the photocatalyst surface and oxidise the water molecule producing hydroxyl radicals. Alternatively, the electrons in the conduction band migrate to the photocatalyst surface and causes reduction to take place by reducing atmospheric oxygen producing superoxide radicals [101]. The hydroxyl and superoxide radicals produced from the redox reactions are strongly reactive and help in breaking down the pollutants or compounds into elementary forms including wastewater treatment [101].

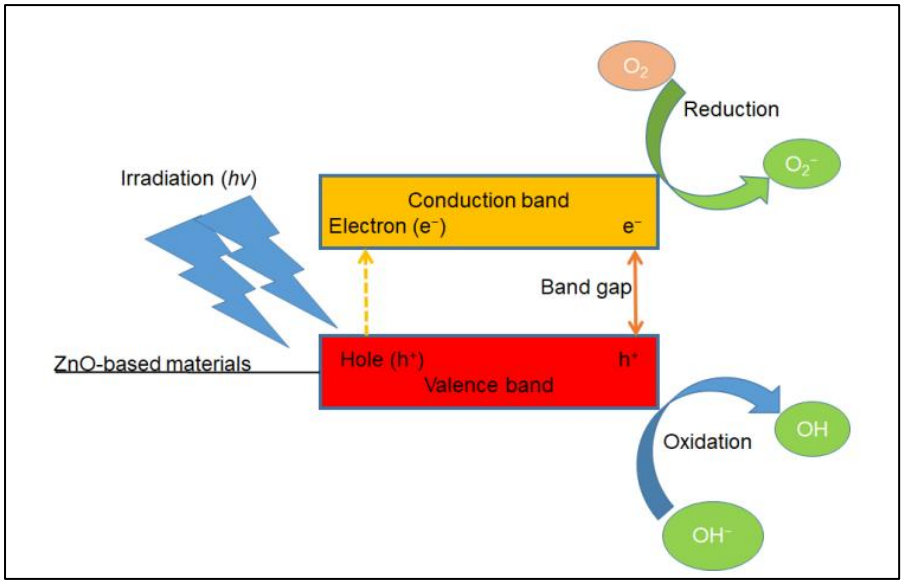

Figure 8. A schematic representation of the photocatalytic mechanism [101]

2.8. Applications of photocatalytic processes

2.8.1. Photocatalytic reduction of carbon dioxide

The carbon dioxide (CO_2) produced as a result of burning fossil fuels, trap heat in the earth atmosphere warming it up and this is what is called global warming. Numerous strategies for instance the capturing, storing, and utilising CO_2 are being developed to minimise the carbon dioxide content in the earth atmosphere [102]. The transformation of CO_2 into useful chemicals product is a great approach to overcome the availability of excess carbon dioxide; however, the double bond (C=O) in CO_2 makes it a highly stable compound that is difficult to break down, consequently complicating this strategy. To resolve this obstacle the application of the photocatalysis process has been considered by a lot of investigators [102].

Iron cobalt disulphide-cobalt disulphide (**$FeCoS_2$-CoS_2**) bilayer nanotubes were produced by Wang et al. (2020) to reduce carbon dioxide using the photocatalytic method. The two metal sulphides were carefully integrated into a double-shelled

tubular heterostructure using the synthetic approach, which involves two-step cation-exchange processes [103]. Both shells are built from incredibly thin two-dimensional (2D) nanosheets, plus the power needed to activate the electron-hole pairs was decreased by utilising the $FeCoS_2$-CoS_2 hybrid structure, and the division was enhanced [103]. Moreover, the structure improved CO_2 adhesion to the surface and the harvest of solar radiation due to its ability to display a large surface area. In summary, these double-shelled nanotubes demonstrated superior durability for photoactive depletion of CO_2 under anaerobic conditions and enhanced photocatalytic activities [103].

2.8.2. Degradation of organic dyes

Among the most common types of contaminants discharged into wastewater from textile and other industrial operations are organic dyes and because the dye is harmful and can be seen in surface water it has raised concern that led to efforts of removing it [104]. Typical biological treatment methods are not capable of removing the dye due to its molecular structure for instance the azo dyes are instead easily converted to toxic aromatic amines under deoxygenated environments and the high salt content in the dye-containing water also affect the productivity of this method [99]. Practices such as dye adhesion and gathering are also utilised to remove the dyes from the water; however, this approach does not result in complete disintegration of the dye, but the formation of additional pollutants [99, 104].

Lately, advanced oxidation processes have been of considerable interest for the complete destruction of dyes and a significant technique resulting in the absolute degradation of many pollutants, involving organic dyes is heterogeneous photocatalysis [105]. Studies have been carried out to investigate the heterogeneous photocatalytic degradation of reactive orange four and reactive black five dyes. The

various semiconductor, TiO_2 and ZnO were used as photocatalysts, and the ZnO degradation results under ultraviolet irradiation were better in contrast to when TiO_2 was employed under the same conditions [99]. A high degradation efficiencies of the RO4 and RB5 dyes were attained with ZnO in a short amount of time; however, these were not the same results for TiO_2 photocatalyst [99].

2.8.3. Solar energy

The sun as part of the solar system provide energy to the earth in the form of light and this energy is given out as particles called photons. This light energy is more than enough for human applications and storage for rainy days. Solar cells utilise a lot of photocatalytic materials to capture sunlight and produce electricity. Numerous sort of solar cells have been invented to exploit solar energy including hybrid, photoelectrochemical, chromatic, and organic cells [99]. Without the availability of well established and effective photocatalysts, solar energy can be utilised in different photovoltaic devices for a satisfactory and efficient conversion of sunlight into solar energy for broad utilisation in various fields [62]. Apart from the sole conversion and storage of sun light, it may also be harvested and used to clean up the environment through pollutants decomposition [62].

2.8.4. Water and wastewater treatment

The process of photocatalysis can be used to break down toxic compounds in water making use of sunlight as a source of energy [93]. The main advantage of photocatalysis in the degradation of harmful substances is that end products such as carbon dioxide (CO_2), water (H_2O), and inorganic salts are produced, and no additional toxic products are given off. This aspect is important with regard to the undesired potential impact of photocatalysis on the environment [94]. This is the primary purpose for the current study on photocatalysis utilisation in hydrogen energy

production and environmental remediation. Water resources have been increasingly contaminated by different types of pollutants in recent decades, which has led to research into photocatalytic techniques for the removal of the different pollutants [45, 99].

2.8.5. Water splitting

Photocatalysis or photoelectrochemical water splitting techniques can be employed in the splitting of water into oxygen and hydrogen using solar energy [1, 10]. This technique dates back to 1972 when Fujishima and Honda used TiO_2 semiconductor as an electrode to perform the splitting of water in a PEC [45]. The procedures of photocatalytic water splitting involve the irradiation of the semiconductor photocatalyst with light to activate it. The electrons in the irradiate materials absorb the light and are excited from the valence band to the conduction band resulting in the electrons in the conduction band and holes in the valence band. Both the photogenerated holes and electrons moves to the photocatalyst surface and react with the molecules of water in solution producing oxygen and hydrogen through the oxidation and reduction reactions taking place on the anode and cathode, respectively [1]. These procedures for the photocatalytic water splitting are identical to that of the process of photocatalysis.

2.9. Characterisation of the fabricated ZnO thin films

2.9.1. Fourier-transform infrared (FTIR) spectroscopy analysis

Fourier transform infrared (FTIR) spectroscopy is a widely utilised identification technique of the functional groups in the solid, liquid, and/or gas materials by employing the gleam of infrared radiations [106]. The instrument used is called an

FTIR spectrometer, generally composed of a sample compartment, an infrared (IR) light source, an amplifier, an interferometer, a detector, and a computer [106]. The Fourier transform infrared spectroscopy working principle is that the infrared light is absorbed by the molecules at specific frequencies, which correlate to the vibrational modes of their chemical bonds [107]. A molecular fingerprint is generated by the ensuing absorption spectrum, which makes it possible for the characterisation and identification of a range of inorganic and organic materials [107]. For analytical reasons the highly utilised spectral region is the mid-infrared (mid-IR), in the range 4000 – 400 cm^{-1}, because it contains the characteristic bands for identification and is what is commonly regarded as IR spectroscopy [107].

The molecule being analysed should be able to absorb IR light (IR active) for the functional group determination [106]. A molecule being IR active means that it has a measure of the separation of positive and negative charges [107]. For instance, a single atom does not absorb IR radiation, as it has no chemical bond. Symmetrical molecules like hydrogen (H_2) also do not absorb IR radiation because of a zero dipole moment; however, H-F (hydrogen fluoride) is an IR-active molecule [106]. The interaction between the IR radiation and the covalent bond of the materials with an electric dipole leads to absorption of energy by the molecule, and the bond begins a forth-and-back vibration. Hence, the vibration that produced the alteration in the net dipole moment of the molecule had to absorb IR radiations [106, 107].

The FTIR can provide information such as the identification of unknown materials, it can verify the consistency or quality of a sample, and it can also determine the content of components in a mixture [108]. Some of the major benefits of FTIR are measurement speed; most measurements by FTIR are made in a matter of seconds

rather than several minutes. Sensitivity is greatly enhanced with FTIR because the detectors used are very sensitive, the optical throughput is much raised, which leads to much reduced noise levels, and the rapid scans allow the coaddition of various scans in order to decrease the random measurement noise to any desired level. Finally, the instruments are self-calibrating and never need to be calibrated by the user [108].

2.9.2. X-ray Diffractometer (XRD)

X-ray diffraction (XRD) is a versatile non-destructive analytical method utilised to analyse physical properties such as phase composition, crystal structure and orientation of powder, solid and liquid samples [109]. The XRD principle is that when the X-rays strike solid materials, they scatter due to the electrons revolving around the nucleus of atoms. These scattered waves, emitted in multiple directions, interfere with each other [110]. The interference can be destructive or constructive, based on the direction type of interaction of waves. There is a strong connection between diffraction and periodicity; shorter diffraction angles are observed with higher periodicity and vice versa [110]. The absence of a periodic arrangement in amorphous materials results in the XRD graph only indicating the highest average peak at a precise diffraction angle, whereas crystalline materials show diverse prominent XRD peaks due to the periodic arrangement of atoms [110].

By comparing the XRD pattern obtained from an unknown sample with patterns of a reference database, identification of faces is achieved. The broadest database is maintained by the International Centre of Diffraction Data (ICDD). On the other hand, it is possible to build up a reference database from experimental diffraction patterns of pure faces and/or patterns published in the scientific literature or derived from one's

own measurements. Qualitative and quantitative phase analysis of pure substances and mixtures are the main uses of XRD [109]. The most common technique for phase analysis is often called X-ray powder diffraction, and the analysis of phase alters under other special conditions such as temperature, humidity and applied pressure. Analysis of physical features such as crystal orientation, crystallite size, and residual stress is called the ‘microstructure’ of polycrystalline materials. A lot of these techniques can also be used for polycrystalline layered materials such as coatings and thin films using a method called grazing incidence XRD [109].

CHAPTER 3: RESEARCH METHODS

3.1. Research design

The research design below illustrates the steps that were followed in this study. In order to achieve successful results, the steps were carried out in the order that they appear (1-4). The preparation of precursor solutions and the fabrication of thin films were done as per the procedures described in [25].

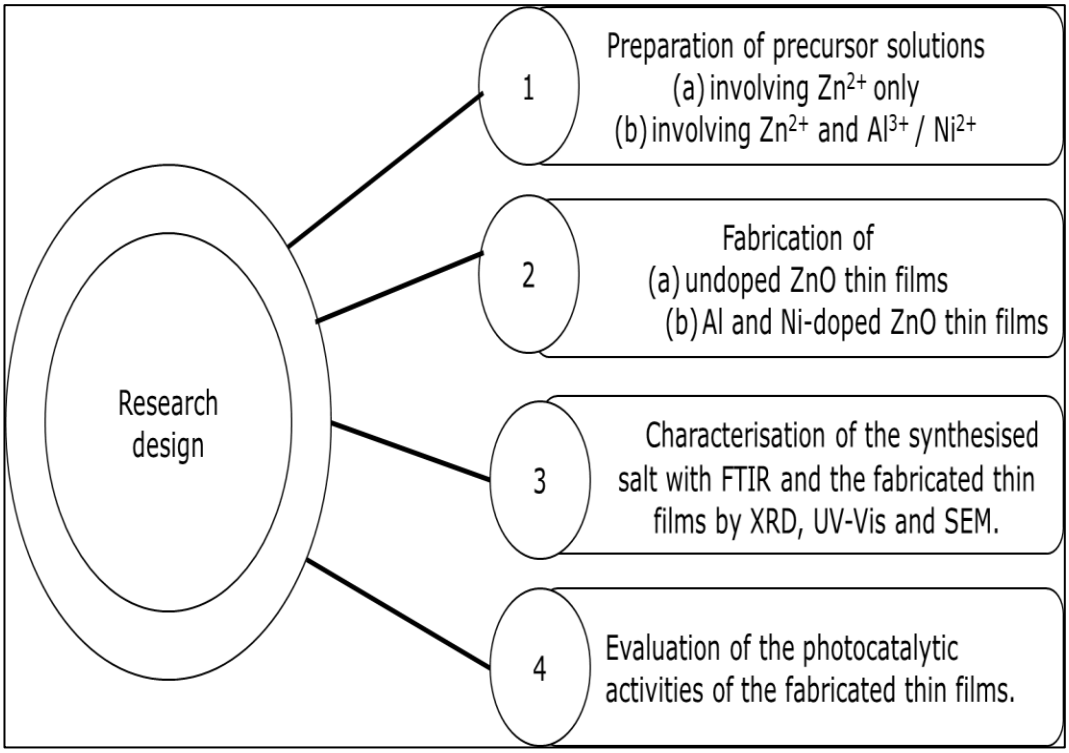

Figure 9. Research design outlining the steps that were followed in this study

3.1. Procedures

3.1.1. Materials

Ammonium aluminium oxalate ($(NH_4)_3$ Al $(C_2O_4)_3$) was synthesised in this research according to the procedures described in [111]. Zinc acetate dihydrate ($Zn(CH_3COO)_2{\cdot}2H_2O$), distilled water, 2-propanol, nickel acetate tetrahydrate ($Ni(CH_3COO)_2{\cdot}4H_2O$), and ammonium hydroxide solution (25% NH_3) were available in

the laboratory. The quartz glass substrates with proportions of 100 × 100 × 1.6 mm^3 were bought from Akishima Glass Co., Ltd. In Tokyo, Japan, they were cut into 20 × 20 mm^2 sizes and cleaned ultrasonically for half an hour with a water-detergent mixture. They were then rinsed multiple times with distilled water and lastly with 2-propanol. All chemical reagents were utilised with no additional purification.

3.1.2. The synthesis of ammonium aluminium oxalate complex [111]

Aluminium hydroxide (2.0356 g, 0.0261 mol) and oxalic acid (6.0164 g, 0668 mol) were dissolved with 50.7216 ml of distilled water in a 250 ml beaker using a stirring rod. This mixture (volume A) was then refluxed for 1 hour at 90 ℃, and the residues were filtered off by gravity. The filtrate was left to cool, and its volume was measured and recorded as volume B (70 ml). 140 ml of ethanol was added to the filtrate as per the ratio (2:1) of ethanol to volume B while stirring with a magnetic stirring bar. 20 ml of ammonium hydroxide was then added dropwise until the solution was basic, as tested with the litmus paper. The product was filtered through Buchner filtration and dried in a desiccator to give an actual yield of 5.7250 g.

Figure 10. The synthesised salt of ammonium aluminium oxalate complex

3.1.3. Preparation of precursor solution/s involving Zn^{2+} complexes only

The coating solution involving Zn^{2+} complexes only was prepared by dissolving zinc acetate dihydrate (0.4975 g, 2.267 mmol) in 20.00 g of distilled water, followed by adding 25% ammonium hydroxide solution (2.1766 g, 32 mmol NH_3). The mixture was stirred for one hour at room temperature on a magnetic stirrer with a magnetic stirring bar. The total concentration of Zn^{2+} ions in the precursor solution was 0.10 mmol g^{-1}. The figure below is a representation of any of these solutions that were prepared.

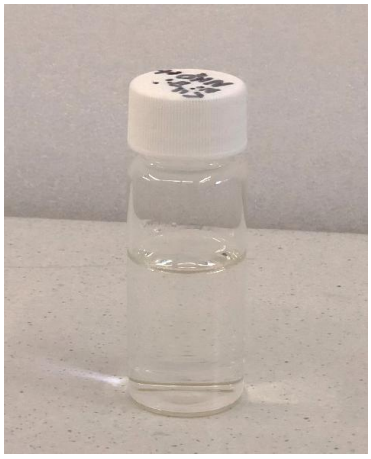

Figure 11. Prepared solution containing Zn^{2+} complexes only

3.1.4. Preparation of precursor solutions involving Zn^{2+} and Al^{3+} complexes

The coating solutions involving Zn^{2+} and Al^{3+} complexes were prepared by mixing different quantities (2%, 4%, and 8%) of ammonium aluminium oxalate with zinc acetate dihydrate in 20.00 g of distilled water, followed by the addition of 25% ammonium hydroxide. The grams of zinc acetate dihydrate and ammonium aluminium oxalate that were used varied with each doping mole percentage of aluminium. The mixtures were stirred for one hour on a magnetic stirrer using a magnetic stirring bar at room temperature. The total concentration of Zn^{2+} ions in each coating solution prepared was 0.10 mmol g^{-1}.

Precursor solutions involving Zn^{2+} and Al^{3+} complexes using different doping mole percentages of aluminium were obtained as shown in the figure below. As the doping mole percentages were increased from 8% to 16%, the solutions attained were not well dissolved, making them unsuitable for spray-coating; hence an 8% doped solution was the end point for this dopant.

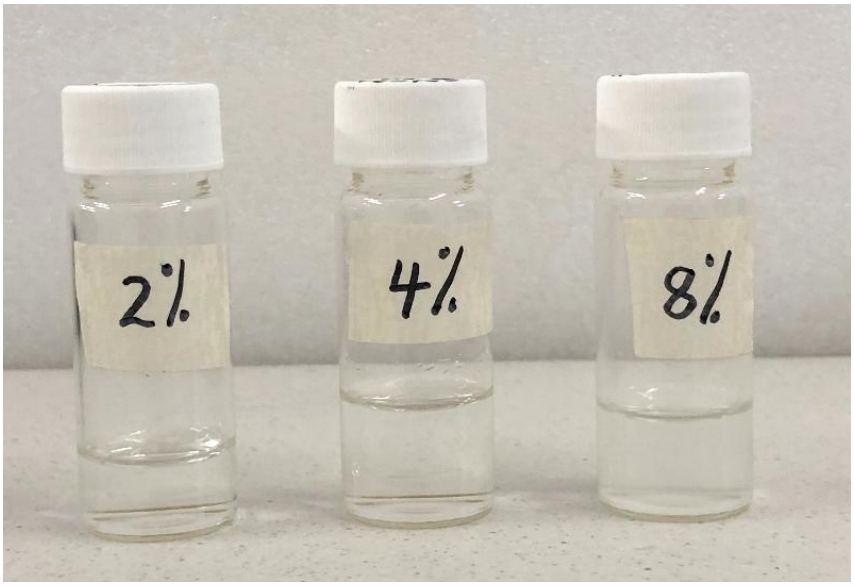

Figure 12. Precursor solutions involving Zn^{2+} and Al^{3+} complexes

3.1.5. Preparation of precursor solutions involving Zn^{2+} and Ni^{2+} complexes

The coating solutions involving Zn^{2+} and Ni^{2+} complexes were prepared by mixing different quantities (2%, 4%, 8%, and 16%) of nickel acetate tetrahydrate with zinc acetate dihydrate in 20.00 g of distilled water, followed by the addition of 25% ammonium hydroxide. The grams of zinc acetate dihydrate and nickel acetate tetrahydrate that were used varied with each doping mole percentage of nickel. For one hour, the mixtures were stirred on a magnetic stirrer using a magnetic stirring bar at room temperature to obtain well-dissolved precursor solutions, respectively. The total concentration of Zn^{2+} ions in each coating solution prepared was 0.10 mmol g^{-1}.

The figure below shows the precursor solutions involving Zn^{2+} and Ni^{2+} complexes using different doping mole percentages of nickel that were obtained. As the doping mole percentages were raised from 2% to 16%, the colour of the solutions became more concentrated in blue, indicating the presence of more nickel ions in the solutions. As a result of having more nickel ions in solution, the solutions from 32% had poor adhesion on the glass substrate, and 16% doped solution was the end point.

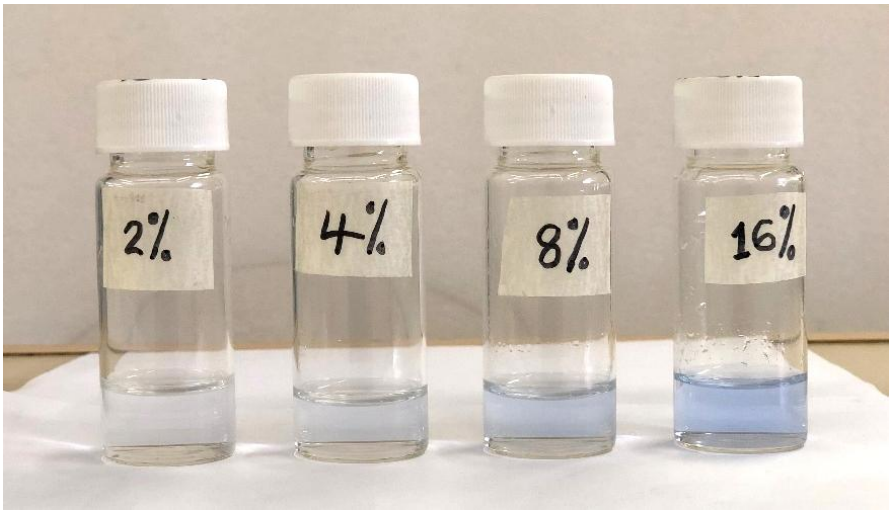

Figure 13. Precursor solutions involving Zn^{2+} and Ni^{2+} complexes

3.1.6. Fabrication of undoped, Al, and Ni-doped ZnO thin films

To fabricate undoped, Al, and Ni-doped ZnO thin films, spray-coating was performed individually onto pre-heated quartz glass substrates of size 20 × 20 mm^2 using either 3 or 6 grams of the above-mentioned precursor solutions for the desired thin film. The temperature of the hot plate was kept at 180 °C and was continuously monitored with a thermocouple. Every precursor solution was sprayed onto a pre-heated quartz-glass substrate from the airbrush, spraying for 5s at 20s intervals using compressed air as a carrier gas. The sprayed films were heat-treated at 450°C for 30 minutes in the air using a furnace to obtain thin films.

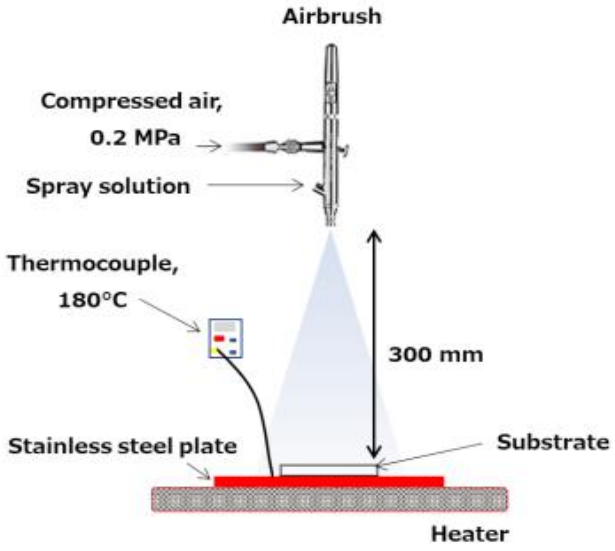

Figure 14. A diagrammatic representation of the spray-coating setup used in this study

3.1.7. Characterisations

The Fourier transform infrared (FTIR) was employed to distinguish the functional groups in oxalic acid and ammonium oxalate, and the product synthesised. The measurements were taken in the IR region of 4000 cm^{-1} to 400 cm^{-1} using the potassium bromide (KBr) pellet method. Prior to FTIR analysis, the samples were mixed with 200 mg of dry KBr powder in the ratio (1:2) of the sample to KBr and finely grind using a mortar and pestle. KBr is IR-transparent and acts as a matrix; the results attained correspond to the vibrational modes of their chemical bonds as the samples absorbed IR light. The fabricated thin films were characterised for their structural properties using the X-ray diffractometer (XRD) instrument (Rigaku Miniflex 600) with Cu K-alpha radiation at a scanning step of 0.01 degrees. To analyse the optical properties of the fabricated thin films as they interact with light in the UV-Vis region of the electromagnetic spectrum, the UV-Vis spectrophotometer was

utilised (using Ocean View software). The main optical properties of interest were the absorbance and transmittance of light and were measured in the wavelength range 200–800 nm. The scanning electron microscope was used to characterise the morphology of the fabricated thin films. The SEM results aid in comprehending the input of grain shape, size, and film uniformity to the overall properties and performance of the thin film.

3.1.8. Investigations on the applicability of the fabricated thin films as photocatalysts

The photocatalytic activities of the fabricated thin films were studied by measuring the aqueous solution of methyl orange (MO) degradation under visible light irradiation. A concentration of 10 mg/L in a 120 ml methyl orange solution was initially used based on literature [36]. However, the concentration was changed to suit the optimum available conditions because not all the conditions in the literature, such as the photocatalyst surface area, light power, and continuous stirring before and after light irradiation, could be implemented. A 120 ml methyl orange solution with a concentration of 2.5 mg/L was then prepared, and 4 ml of this solution was placed in nine catalyst placement sections of the self-designed reactor, respectively. The different thin films were then submerged in the methyl orange solution in different sections of the catalyst placement. The solution was left in the dark for 30 minutes to establish the equilibrium (adsorption-desorption) before irradiating with visible light [19].

To block out any external light, the photocatalytic degradation was performed in a wooden box at room temperature [36]. The reactor consisted of nine light-emitting diodes (LEDs) with visible lights (10 W) in a parallel arrangement and were kept at a

distance of 7.5 cm above the reactor. The irradiated solutions of 4 ml were collected only after 4 hrs of irradiation, and the absorbance was measured using a UV–Vis spectrophotometer for calculating the concentration since absorbance is directly proportional to concentration according to Beer Lambert law. The 4 hours of irradiation were determined primarily by the operating hours of the laboratory where the experiment was conducted, taking into consideration the measurements before and after the experiment, for instance, absorbance measurements of the irradiated solution, allocation and removal of 4 ml solutions to and from the nine catalyst placement sections, housekeeping, and the protection of the used light source from overheating. The procedures were established with reference to the articles [19, 36, 112], adjusted to the available equipment, and finally refined after trials and errors.

CHAPTER 4: RESULTS AND DISCUSSION

4.1. The fabricated thin films

Table 1 below shows the fabricated thin films, where some were fabricated by spray-coating with 3 grams of the corresponding precursor solution for the desired thin film and others with 6 grams and then heat treated. This was done to see the effect of the thickness on the properties of the fabricated thin films. The specific amounts used for spray-coating, 3 and 6 grams, were selected according to the procedures in [87, 88], where the thickness measurements were done on the obtained films fabricated using 3 and 6 grams of precursor solutions, and the thickness values were less than one micrometre, making them thin films. The as-sprayed films were heat-treated to remove organic ligands from metal complexes involved in spray-coating precursor films and for the irreversible phase transformation which results in the formation of thin films of crystallized metal oxides [113]. To identify the effect of the dopant amount, different doping mole percentages were used, and the sequence utilised was using even numbers starting with 2 and then doubling to get the next digit to use, and the stopping point was determined by how well dissolved the solutions attained were as well as the adhesion of these solutions onto the supporting substrate after heat-treating. The doping mole percentages, for example 2% Al does not mean that there is 2 grams of aluminium in solution prepared. Instead it means that in a solution mixture where the total moles of metal ions are equal to 1 (or 100%), 0.02 moles are of aluminium ions and the rest 0.98 moles are of zinc ions. Two different dopants, Al and Ni, were used to evaluate the effects of various dopants on the characteristics of the resultant thin films. For comparison's sake, the samples were fabricated in pairs for all the doping mole percentages.

Table 2. The thin films fabricated through the aqueous-spray coating method

Dopant	Sample name	Doping mole %	Spray-coated with 3 g	Spray-coated with 6 g
Undoped	W1	0	✓	
	W2	0		✓
Aluminium	W3	2	✓	
	W4	2		✓
	W5	4	✓	
	W6	4		✓
	W7	8	✓	
	W8	8		✓
Nickel	W9	2	✓	
	W10	2		✓
	W11	4	✓	
	W12	4		✓
	W13	8	✓	
	W14	8		✓
	W15	16	✓	
	W16	16		✓

4.2. Fourier transform infrared (FTIR) analysis

The FTIR results showed different functional group peaks that appear in the mid-IR region (4000 ~ 200 cm^{-1}), which is in the wavelength range of 4000 – 400 cm^{-1}. In the present study, the C=O, the symmetrical and asymmetrical O-H bonds, and the C-O bonds in the oxalic acid spectrum were identified at wavenumber 3417 cm^{-1}, 725 cm^{-1}, and 1249 cm^{-1}, respectively, with reference to literature [114, 115]. The ammonium oxalate spectrum gives peaks at 2987 cm^{-1}, 1593 cm^{-1}, 1429 cm^{-1} and 1311 cm^{-1} which are allocated to the N-H stretch, C=O, NH_4^+, and C-O bonds, respectively. These

values strongly correspond with the previous reported values [116]. In the product spectrum, the O-H, C=O, NH_4^+, and C-O bonds were identified at wavenumbers 3182 cm^{-1}, 1593 cm^{-1}, 1400 cm^{-1} and 1292 cm^{-1} respectively. A new peak in the product spectrum at wavenumber 772 cm^{-1} is confirmed to be an Al-O bond, with reference to [117, 118]. These findings strongly indicate that the synthesised product is indeed ammonium aluminium oxalate. The figure below presents all the FTIR spectra obtained for the samples.

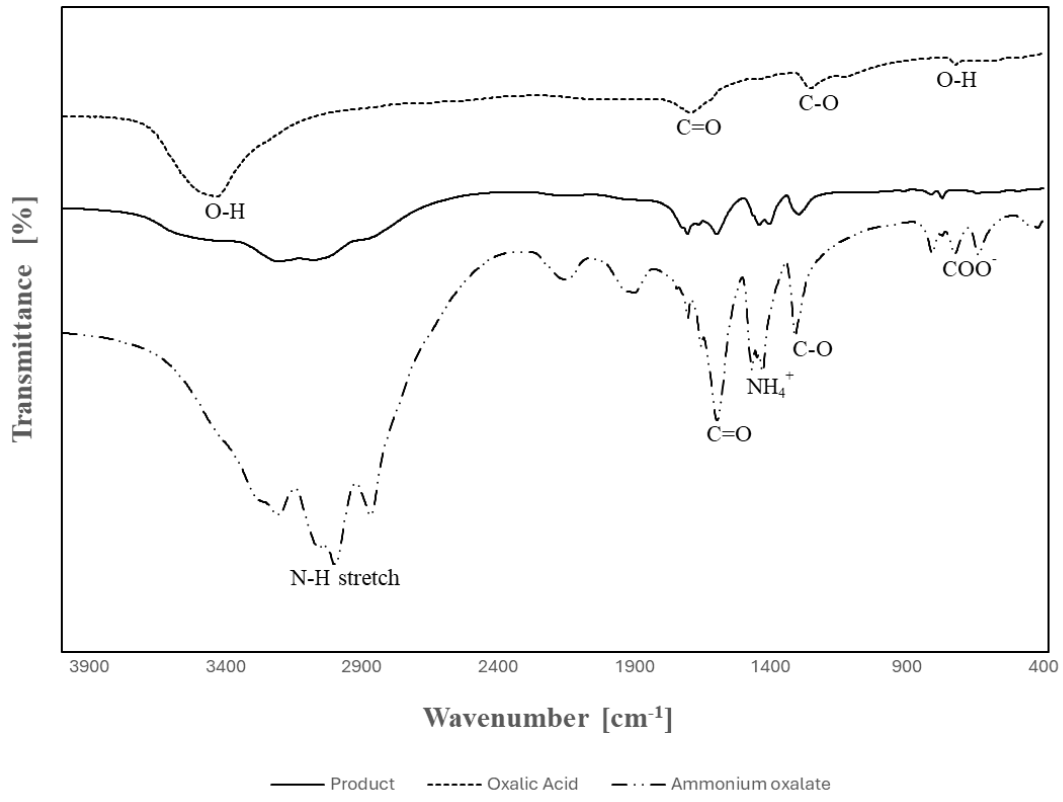

Figure 15. FT-IR spectra of oxalic acid, ammonium oxalate, and the ammonium aluminium oxalate in transmission mode

4.3. Characterisation of the fabricated thin films

4.3.1. Crystal structure characterisation

The X-ray diffractometer (Rigaku Miniflex 600) instrument was used in this study to determine the crystal structure of the fabricated thin films based on the diffraction of x-rays by using Cu K-alpha radiation, with a scanning step of 0.01 degrees in the 2-theta range of 20-80°. The figures below show the XRD patterns of the Al and Ni-doped ZnO thin films spray-coated with 3 and 6 grams of corresponding solutions for the desired thin films.

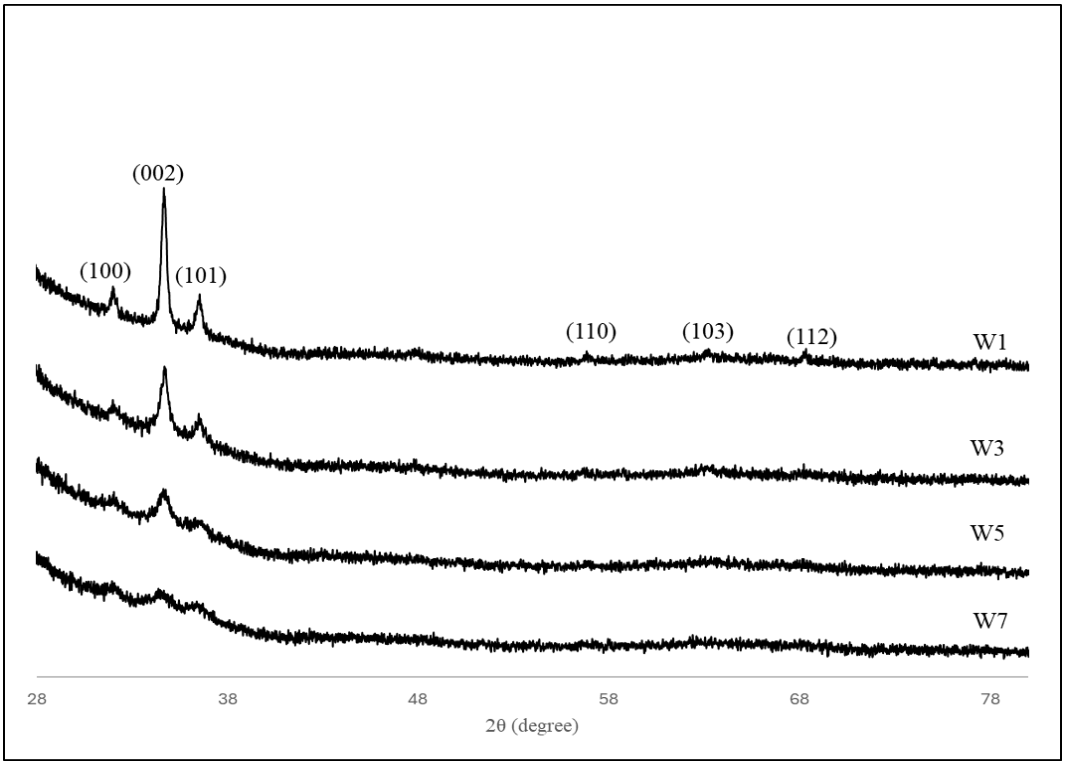

Figure 16. XRD patterns of Al-doped ZnO thin films spray-coated with 3 grams of corresponding solutions for the desired thin film

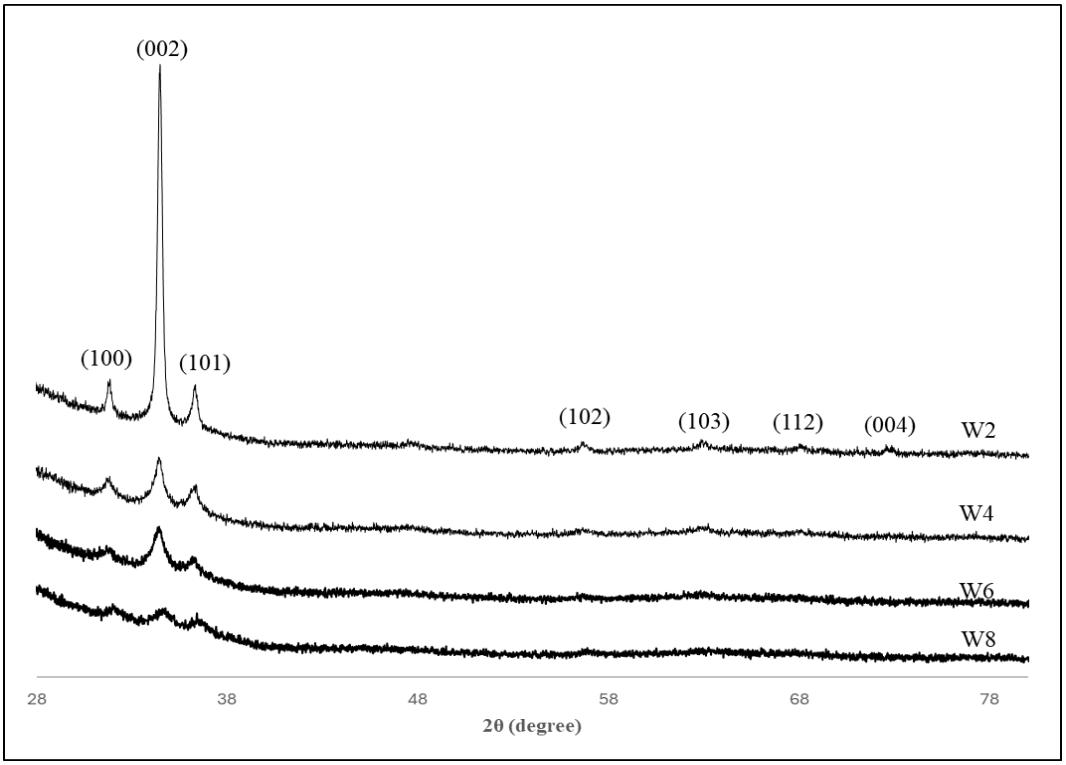

Figure 17. XRD patterns of Al-doped ZnO thin films spray-coated with 6 grams of corresponding solutions for the desired thin film

The figures above illustrate the XRD pattern for the undoped and Al-doped ZnO thin films spray-coated with 3 and 6 grams ranged between 28° and 80°. The several diffraction peaks detected at 2θ = 31.7812°, 34.4295°, 36.2668°, 47.5546°, 62.87611°, and 68.5239° in the undoped ZnO thin films correspond to the (100), (002), (101), (102), (103), (112), and (004) miller indices individually, confirmed by the ICDD card of ZnO (ICDD card number 01-079-5604). The undoped ZnO thin film spray-coated with 6 grams of corresponding solution for the desired thin film has an additional peak at 2θ (degree) = 73.1299° assigned to the (004) plane. The diffraction peaks at 2θ = 47.5546°, 62.87611°, 68.5239°, and 73.2094° designated to the (102), (103), (112), and (004) miller indices are not appearing in the Al-doped ZnO XRD patterns. The presence of more, high and sharp peaks was reported to be a sign of high crystallinity, and with these results, this means that the undoped ZnO thin films are more crystalline

than the Al-doped ZnO thin films [119]. The XRD peaks disappearance towards the higher angles with the doping of Al may be due to the lower ionic radius of Al^{3+} (53 pm) in comparison to that of Zn^{2+} (74 pm); as it substitutes the Zn^{2+} in the crystal lattice, it leads to strain and change in the nature of the crystal lattice [120]. As shown in the figure above, a decrease in the peak intensity and the broadening of peaks were noticed with increasing the doping mole% of Al. When Al impurities are incorporated into the interstitial ZnO lattice site, the crystallinity of the ZnO thin films is decreased, and this is seen in the abrupt decrease in peak intensity and peak broadening with increasing Al dopants. [47, 121]. The broadening of peaks also signifies that the size of the particles of the Al-doped ZnO thin films were reduced compared to those of the undoped ZnO thin films, as stated in reference [122]. The photocatalytic reaction of the Al-doped ZnO thin films may be enhanced by the large surface area that comes from the reduction in crystal sizes [18].

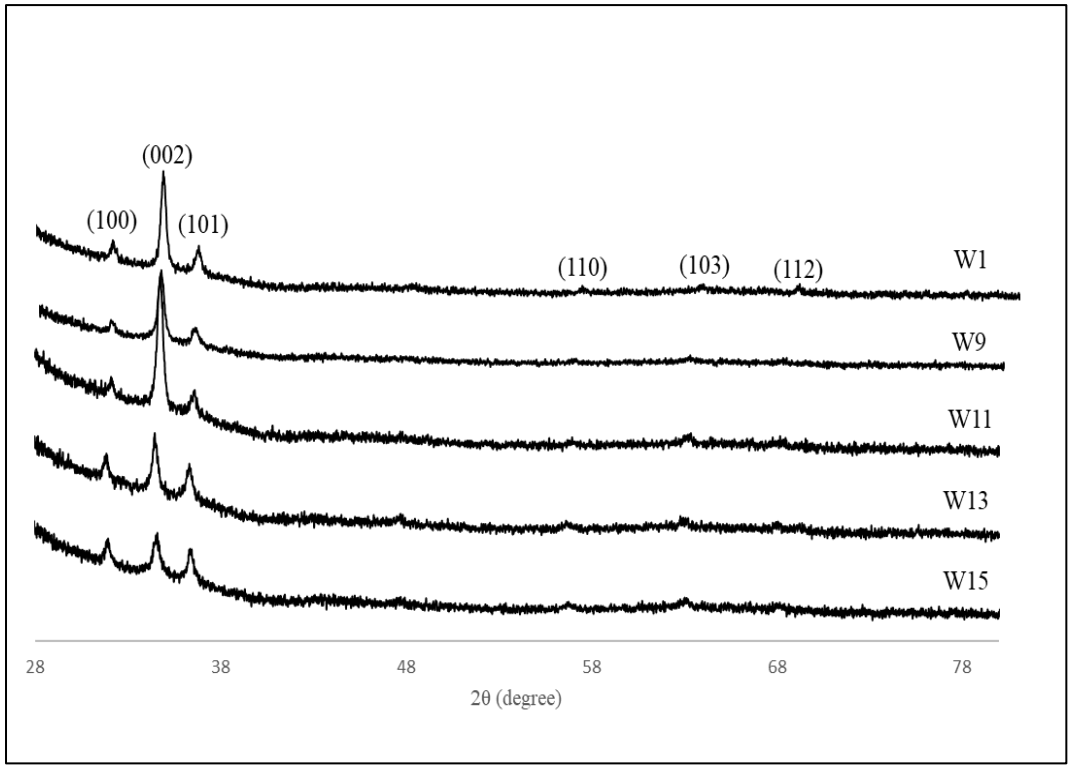

Figure 18. XRD patterns of Ni-doped ZnO thin films spray-coated with 3 grams of corresponding solutions for the desired thin film

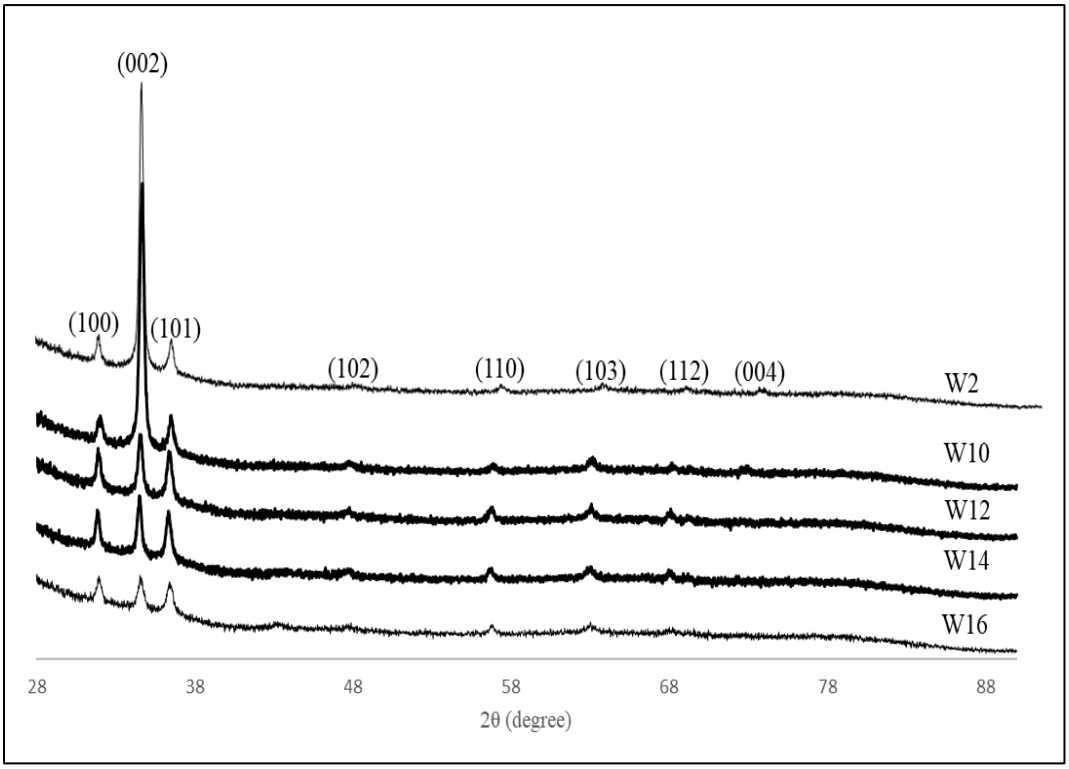

Figure 19. XRD patterns of Ni-doped ZnO thin films spray-coated with 6 grams of corresponding solutions for the desired thin film

The XRD patterns for the undoped ZnO thin films spray-coated with 3 and 6 grams of corresponding solutions for the desired thin films exhibit similar diffraction peaks at 2θ (degree) = 31.8400°, 34.4399°, 36.4100°, 47.9100°, 56.2841°, 62.9799°, and 67.4400° indexed as (100), (002), (101), (102), (110), (103), and (112). The undoped ZnO thin film spray-coated with 6 grams of corresponding solution for the desired thin film has an additional peak at 2θ (degree) = 73.1299° assigned to the (004) plane. Some peaks were observed to disappear in the XRD patterns for the Ni-doped ZnO thin films, with the peak at 2θ (degree) = 73.1299° disappearing in all the Ni-doped ZnO thin films spray-coated with 6 grams of corresponding solution for the desired thin films. The peaks at 2θ = 47.9100° and 67.4400° were observed to disappear in all the Ni-doped ZnO thin films spray-coated with 3 grams of corresponding solutions for the desired thin films. The peaks at 2θ (degree) = 47.9100° and 67.4400° disappeared

only in the 16% Ni-doped ZnO thin film spray-coated with 6 grams of corresponding solutions for the desired thin films. It was found that the samples have a hexagonal wurtzite structure, confirmed by the ICDD card of ZnO (ICDD card number 01-079-5604). The most intense peak for both undoped and Ni-doped ZnO thin films assignable to the (002) plane correlates to the preferred orientation of the zinc oxide hexagonal wurtzite phase [19]. The availability of sharp and high peaks in the fabricated thin films exhibits their well-crystalline nature, and the many peaks indicate their polycrystalline character [119, 123]. The thin films spray-coated with 6 grams of solutions show that they are more crystalline than the ones spray-coated with 3 grams of solutions. The peaks broadening was observed with an increase in nickel doping amount. It was reported that distinctive crystalline structures exhibit varying XRD patterns; this signal changes in the crystal lattice due to doping of nickel into the ZnO lattice [19]. The intensity of the Ni-doped ZnO thin film peaks decreased gradually with an increase in doping amounts of Ni, and the disappearance of peaks ((112), (004)) was observed. The gradual change in width, and intensity of the peaks could be an indicator of successful doping of ZnO structure with Ni [47]. In summary, the XRD results show that the undoped thin films are more crystalline than all the doped thin films, but the Ni-doped ZnO thin films are more crystalline than the Al-doped ZnO thin films.

4.3.2. Optical properties characterisation

The UV-vis spectrophotometer was used to analyse the optical properties of the fabricated thin films as they interact with light in the UV-Vis region (of wavelength 200 nm–800 nm) of the electromagnetic spectrum. The primary optical properties of focus were the absorbance and transmittance of light, and these results are interpreted

below.

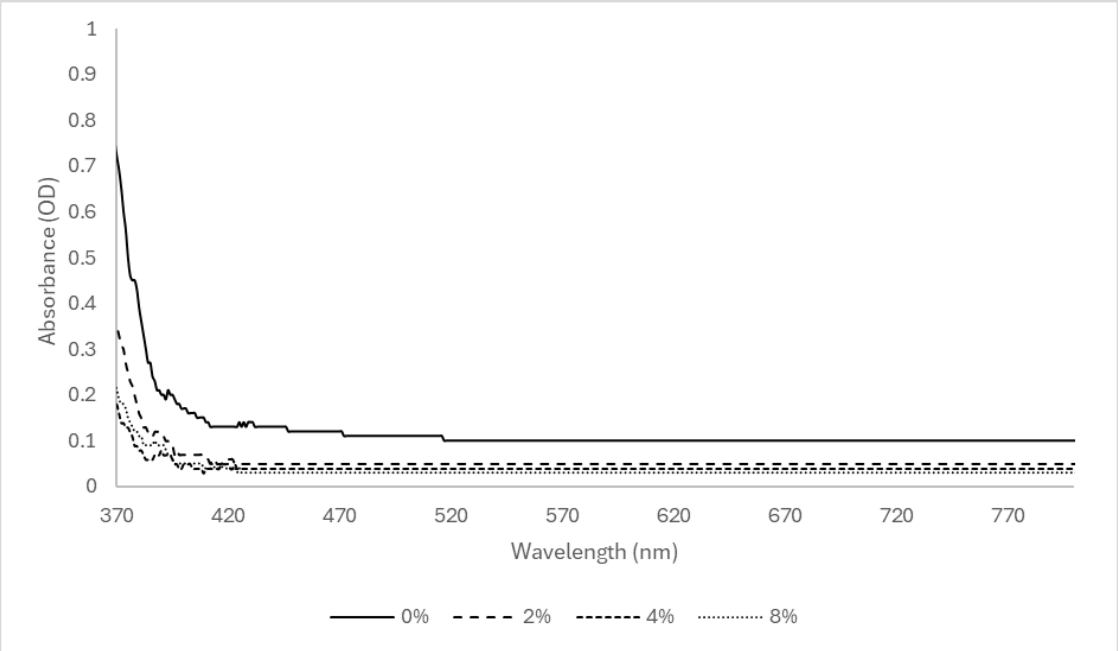

Figure 20. Absorbance spectra of Al-doped ZnO thin films spray-coated with 3 grams of the corresponding solutions for the desired thin films

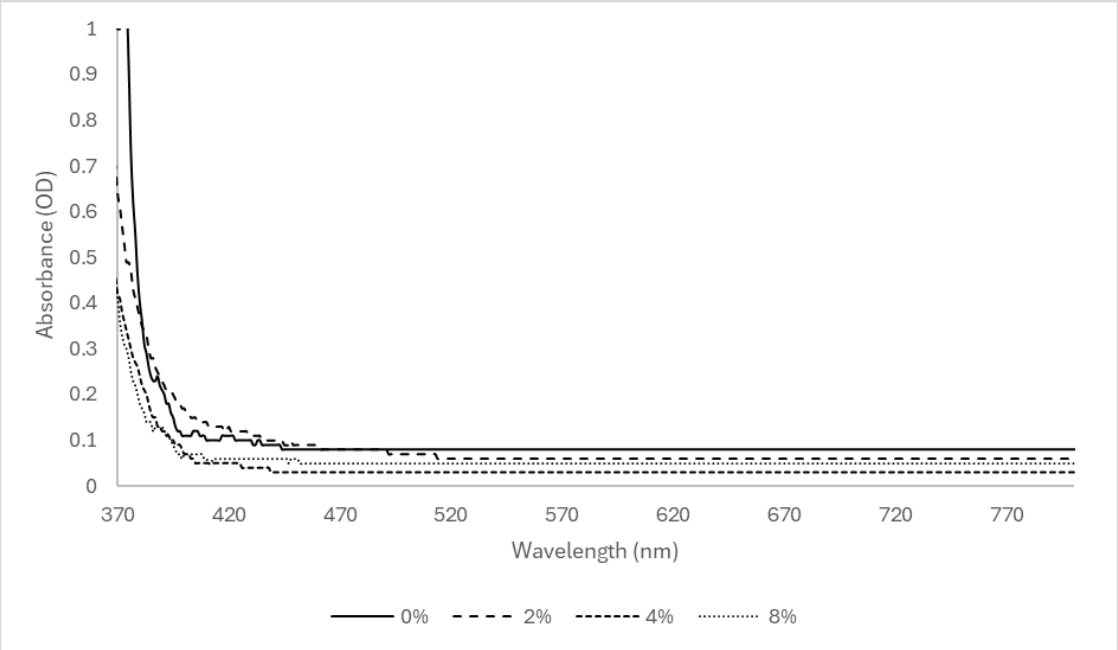

Figure 21. Absorbance spectra of Al-doped ZnO thin films spray-coated with 6 grams of the corresponding solutions for the desired thin films

The figures above portray that all the Al-doped ZnO thin films are absorbing light in the visible region of range 400 nm–800 nm. The thin films spray-coated with 3 grams exhibit low absorption intensity compared to the ones spray-coated with 6 grams, and this is an indication that the amount of solution used during the spray-coating process affects how much light the thin films absorb. In this instance, the more the solution used for spray-coating, the more the light is absorbed by the resultant thin film. The same outcomes were reported in [124, 125]; the author specifically highlighted that the transmittance relies on the thickness of the thin films and also on the metal ions on the thin films, where generally the transmittance is expected to be low for thin films rich in metals [125]. However, the uneven distributions of metal ions onto the substrates may lead to different results. Additionally, the temperature at which the thin film was heated affects its thickness, surface roughness and crystal sizes and overall affects light absorption or transmittance [124]. As the doping amount of Al was increased, the absorbance was observed to decrease for all Al-doped ZnO thin films; the same phenomenon was documented in [126]. The Al-doped ZnO thin films spray-coated with 3 grams are observed to have a much lower absorption intensity in comparison to the undoped ZnO thin film; however, this was not noticed for the thin films spray-coated with 6 grams. This may be due to the uneven thickness of the thin films and the uneven distribution of the solution containing Al complexes onto the supporting substrate. Both Al-doped ZnO thin films spray-coated with 3 and 6 grams of corresponding precursor solutions have a pronounced absorption edge at 370 nm, and they show a shift to the lower wavelength, which is the blue shift. The shift of absorption spectra to shorter wavelengths with higher Al doping mole% indicates that the band gap levels of the Al-doped ZnO thin films have widened [21]. Reports suggest that aluminium impurities in the conduction band influence the blue shift as doping,

with aluminium introduces new electrons or electron traps, and if they occupy the lower level of the conduction band, the band gap size changes [21]. The trend in the absorption of light by the fabricated Al-doped ZnO thin films could be an indication of a successful doping of ZnO with Al.

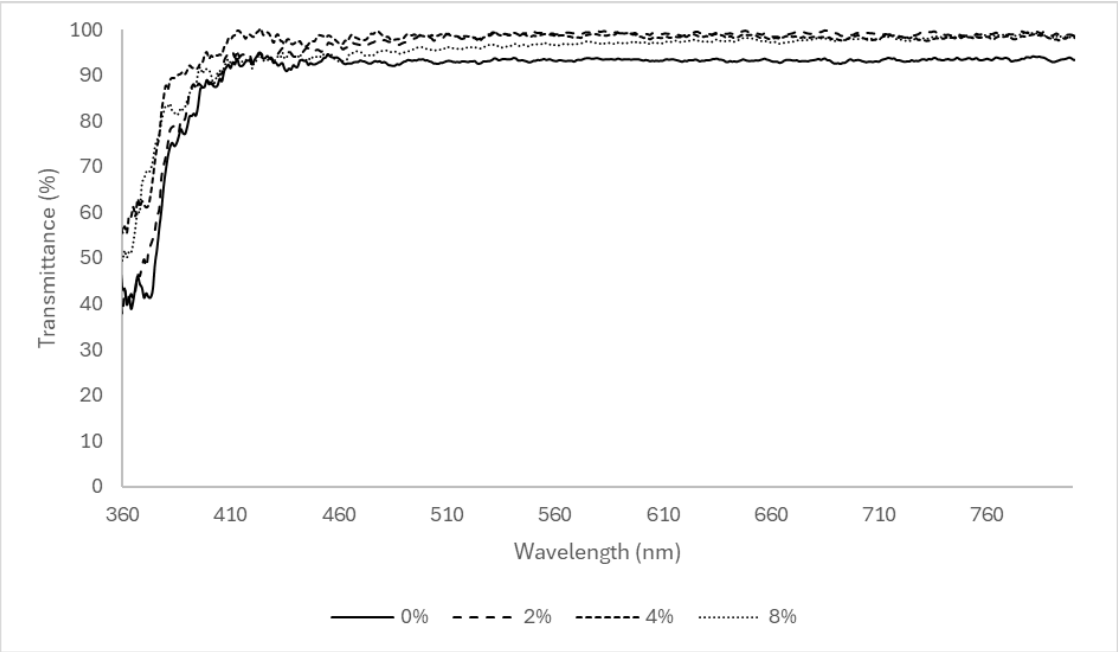

Figure 22. Transmittance spectra of Al-doped ZnO thin films spray-coated with 3 grams of the corresponding solutions for the desired thin films

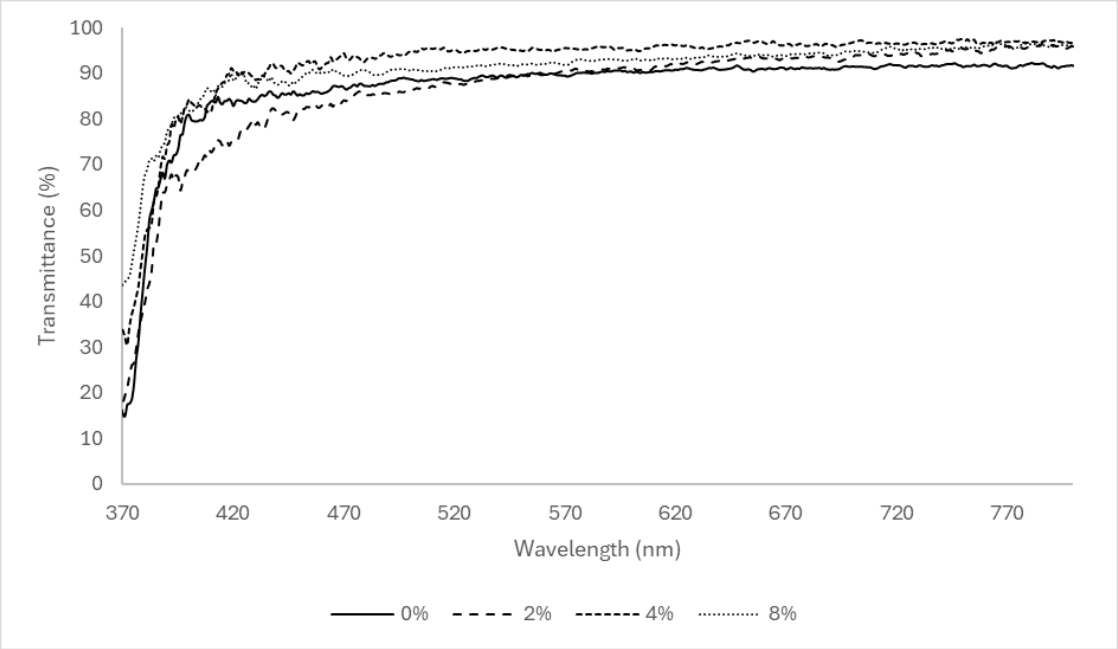

Figure 23. Transmittance spectra of Al-doped ZnO thin films spray-coated with 6 grams of the corresponding solutions for the desired thin films

As shown in the figures above, the transmittance of the Al-doped ZnO thin films spray-coated with 3 and 6 grams of corresponding solutions shows the opposite nature of absorbance, as anticipated. The transmittance was observed to be low at short wavelengths, and it increased with the wavelength values and became steady from 700 nm and beyond. This outcome may be caused by the interaction of the thin films with light at different wavelengths [127]. The 4% Al-doped ZnO thin films spray-coated with 3 and 6 grams of corresponding solution were observed to exhibit a higher transmittance than the 8% Al-doped ZnO thin films in the visible region, and this could be due to the uneven thickness of the thin films. All the thin films demonstrate a great transmittance of visible light that is beyond 80%. The even distribution of thin film materials results in fewer gaps in the samples, which can lead to an increase in visible transmission of these samples [128]. Additionally, the structural properties revealed that the thin films are crystalline, which may be another possible reason for less light

scattering arising in the high transmittance of Al-doped ZnO thin films [18]. The high transmittance of the samples at visible wavelengths makes them suitable for use in photovoltaic devices. For instance, ZnO thin films doped with aluminium are utilised above and/or below as transparent window layers in copper indium gallium selenide thin film solar cells for dirt and corrosion protection [129].

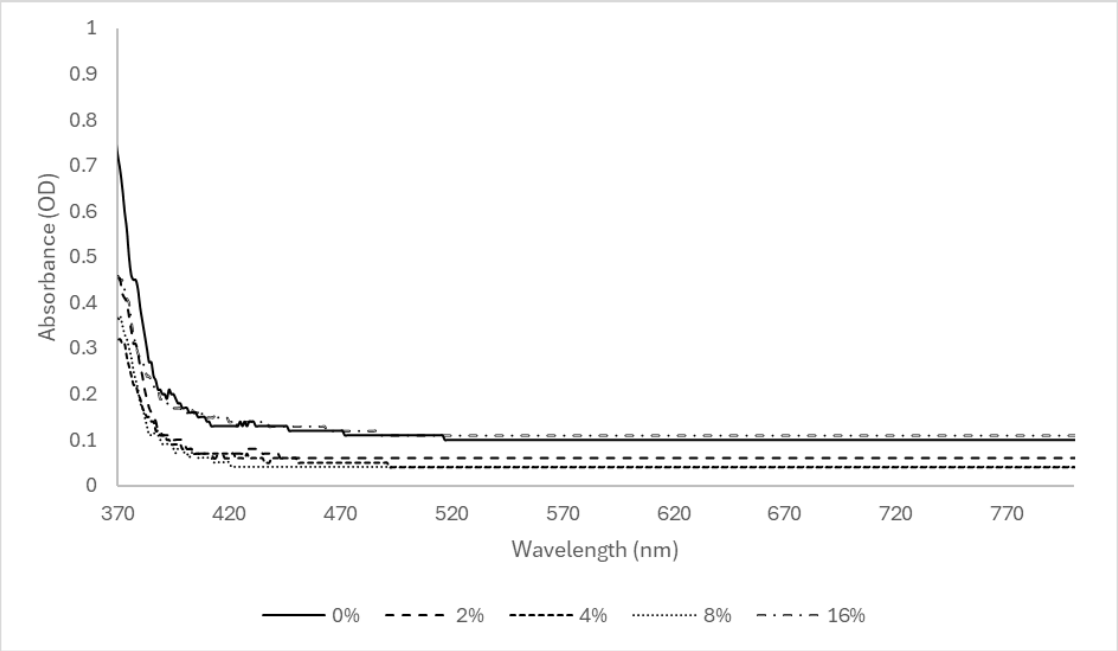

Figure 24. Absorbance spectra of Ni-doped ZnO thin films spray-coated with 3 grams of the corresponding solutions for the desired thin films

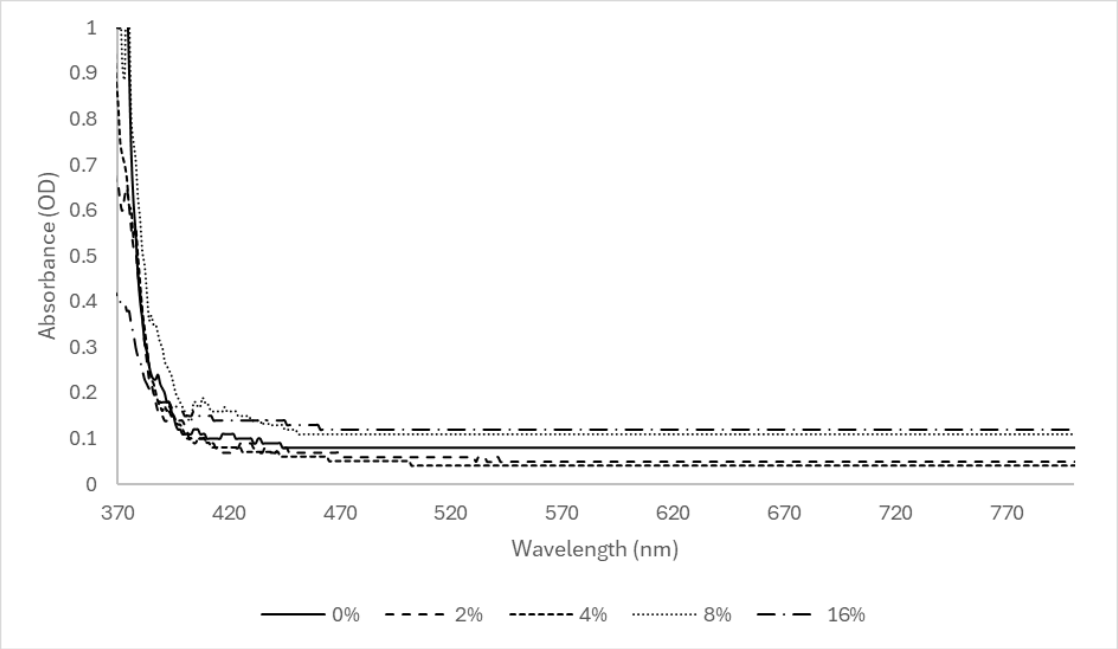

Figure 25. Absorbance spectra of Ni-doped ZnO thin films spray-coated with 6 grams of the corresponding solutions for the desired thin films

As shown in figures 24 and 25 above, all the Ni-doped ZnO thin films are absorbing light in the visible region of range 400 nm–800 nm. The absorbance of light decreases as the Ni doping percentage is increased from 2% to 8% but rises again at 16% Ni content for the thin films spray-coated with 3 grams of respective solutions. On the other hand, the absorbance decreases as the Ni doping percentage is increased from 2% to 4%, yet increases for higher doping levels at 8% and 16% for the thin films spray-coated with 6 grams of respective solutions. This hints that higher amounts of dopant of Ni and spray-coating solution enhance light absorption in these thin films. A greater dopant amount in the solution is likely to promote a more even distribution of dopant complexes, leading to a stronger effect on the absorption of light. The thin film doped with 16% Ni and spray-coated with 6 grams of corresponding solution exhibited the best absorption of light in this study. The absorption edge region of Ni-doped ZnO thin films is situated between 370 nm and 380 nm; in another study it was found to be between 355 nm and 370 nm [54]. A blue shift was observed in the ZnO

thin films after doping with nickel, which conveys that the band gap of the Ni-doped ZnO thin films increased [130]. According to literature, if nickel ions occupy interstitial sites on the ZnO lattice during doping, it enhances light absorption [131].

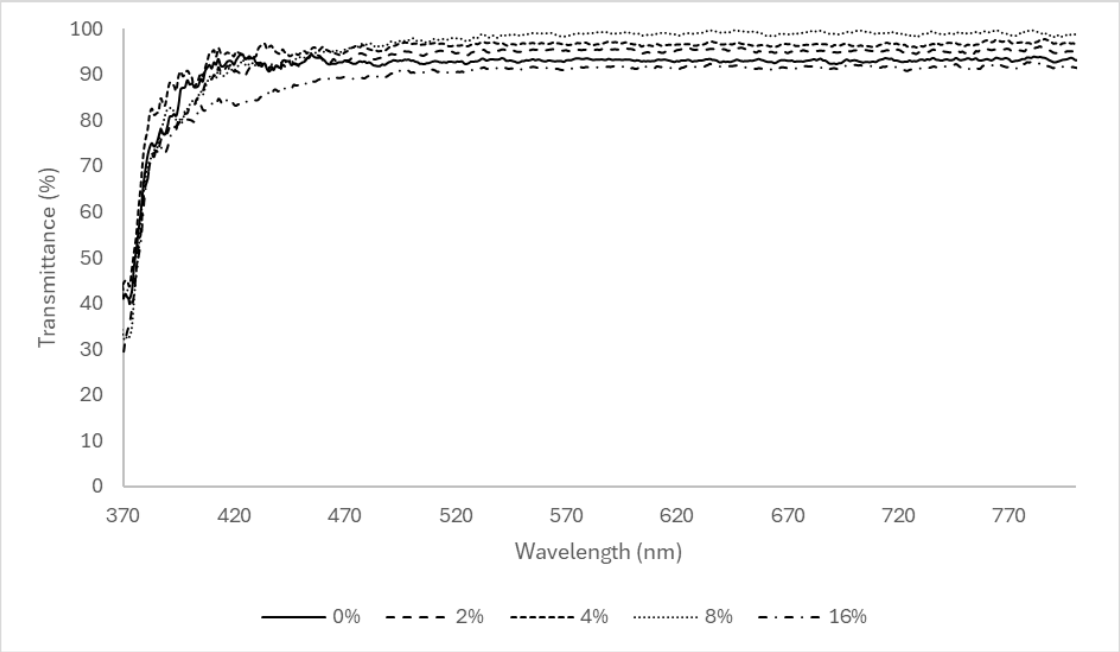

Figure 26. Transmittance spectra of Ni-doped ZnO thin films spray-coated with 3 grams of the corresponding solutions for the desired thin films

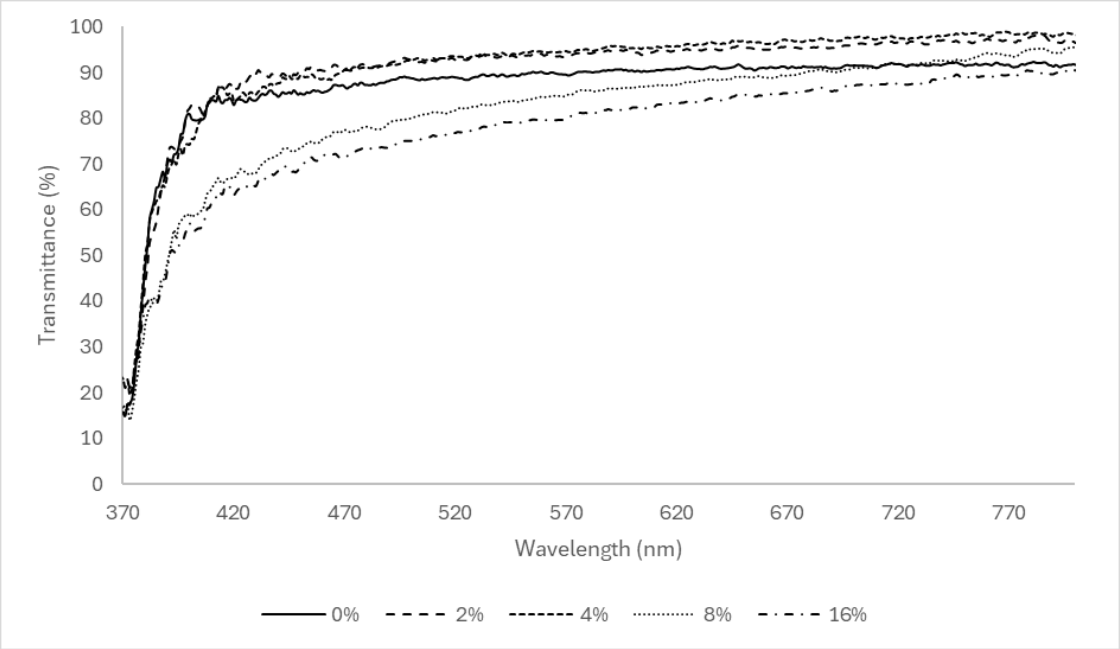

Figure 27. Transmittance spectra of Ni-doped ZnO thin films spray-coated with 6 grams of the corresponding solutions for the desired thin films

The figures 26 and 27 above show that all the thin films exhibit high transparency in the visible range, with transmittance exceeding 70%, even after Ni doping. However, it was observed that transmittance decreases at higher doping levels (8 and 16% Ni-doped), which is the inverse of absorbance for these thin films. The decrease in transmittance at these doping levels might be due to the high nickel impurities in the crystal lattice of ZnO [131]. The highest transparency of 97% was obtained by 4% Ni-doped thin film in the visible region. The transmittance was observed to increase rapidly in the shorter wavelength region and becomes nearly flat in the longer wavelength range, consistent with the findings reported by [132]. Vinay Gupta and Abhay Mansingh suggest that the transmittance depends on the surface roughness because surface scattering reduces the transmittance of light. The appearance of an almost flat transmittance spectrum indicates low surface roughness, which reduces surface scattering and, as a result, increases the transmittance of light [131].

4.3.3. Surface morphology characterisation

The scanning electron microscope (SEM) was used to observe the morphology of the thin films spray-coated with 6 grams of respective solutions. Only certain thin films (0, 2, and 8% Al and Ni-doped ZnO) spray-coated with 6 grams of solutions were analysed due to economic reasons. The analysis of the thin film surfaces by the SEM makes it possible to confirm the homogeneity of the thin films, observe the shape and size of grains and aggregates, and perform a qualitative analysis of the deposited layers.

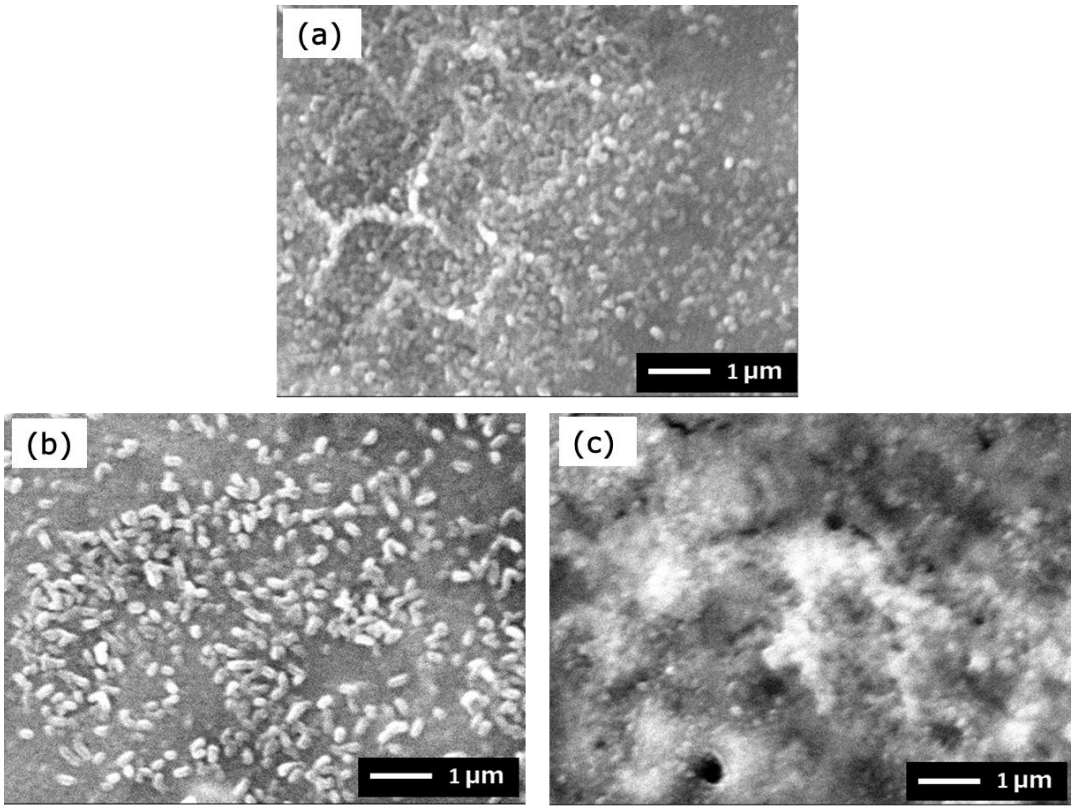

Figure 28. SEM images of (a) undoped ZnO thin film (b) 2% Al-doped ZnO thin film and (c) 8% Al-doped ZnO thin film at the scale of 1 µm

The SEM images of the undoped and Al-doped ZnO thin films at the scale of 1 µm are shown in the figures (a-c) above. The figures show that the undoped and Al-doped ZnO thin films are homogeneously distributed onto the substrates with visible particles

that are not evenly distributed. It is noted that the particle size on these thin film surfaces decreased with the increase in Al doping. This can be attributed to the change in the crystal structure as observed in the XRD results. The particles are also observed to agglomerate with Al-doping, and at 8% Al-doped, the grain boundaries are not visible. According to [128], the creation of stress brought on by the significant difference in ionic radius between zinc and aluminium may be the cause of the change in particle size. While there is no huge difference in the morphology between the undoped and 2% Al-doped ZnO thin films, the 8% Al-doped ZnO shows a noticeable difference in morphology from the two. It was observed that the 8% Al-doped ZnO thin film has a porous surface. The surface containing pores may provide a large surface area and improved photocatalytic activities [133].

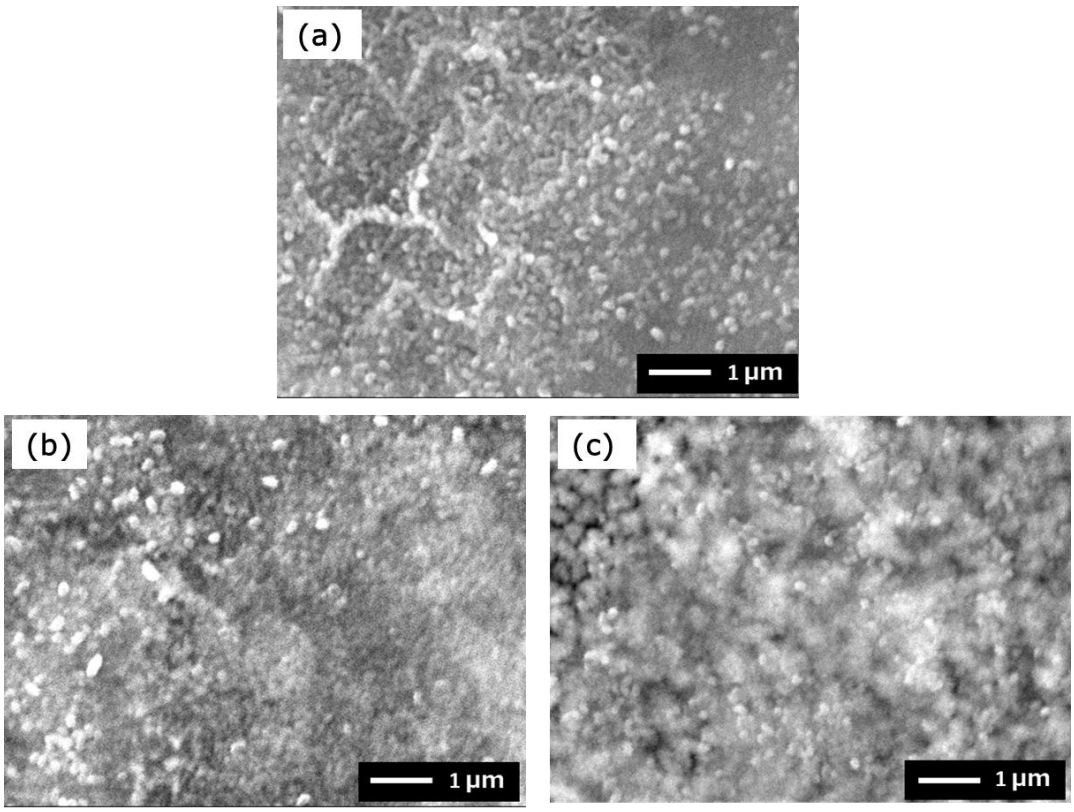

Figure 29. SEM images of (a) undoped ZnO thin film (b) 2% Ni-doped ZnO thin film and (c) 8% Ni-doped ZnO thin film at the scale of 1 µm

The SEM images above show that both the undoped and Ni-doped ZnO thin films are continuously distributed over the entire substrate area without any defects such as voids or cracks, similar to the results reported by [134]. The undoped ZnO thin film shows well-defined particles with distinct boundaries. For the thin film doped with 2% Ni, the particles become smaller with emerging agglomerates. At a higher doping percentage (8% Ni), the thin film surface has poorly defined particles and increased agglomeration. The difference in the morphology of these thin films is an indication that doping nickel ions into the ZnO host lattice modifies the growth route. These results are in correspondence with previous findings [134, 135], where the morphological difference between undoped and Ni-doped ZnO thin films was explained.

4.4. Photocatalytic activity experiment

The figures below show the UV-Vis absorbance readings that were obtained for the different MO dye solutions degraded using various thin film photocatalysts fabricated in this study. The maximum absorption peak for methyl orange in UV-Vis, as shown on the figures below, was at 464 nm, in agreement with [136].

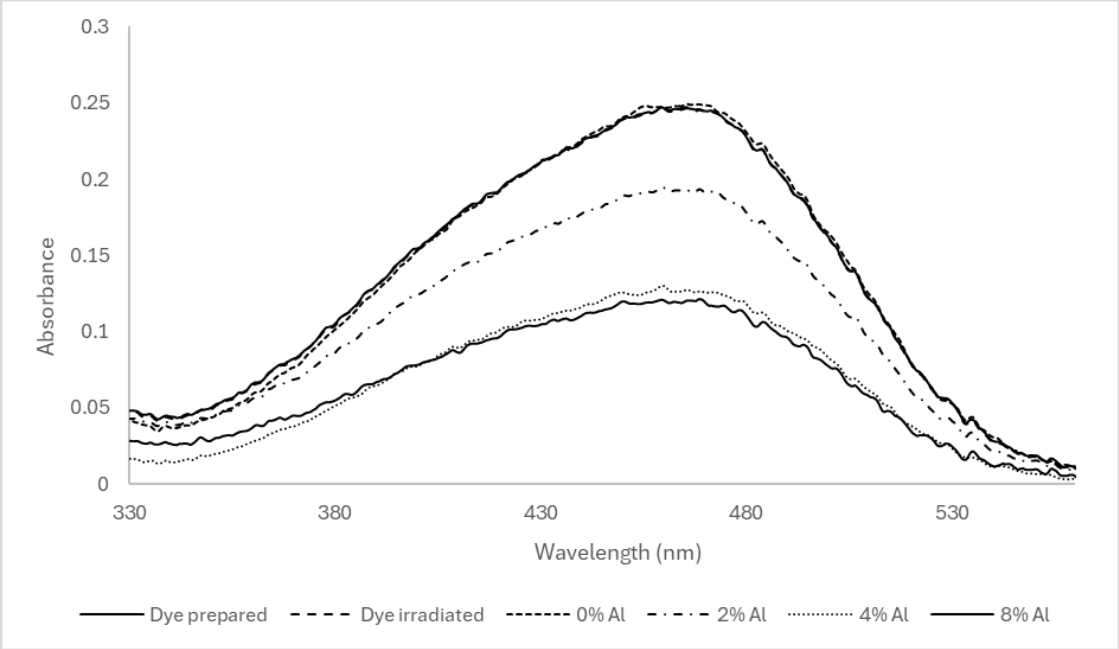

Figure 30. Absorbance spectra for the decomposition of 2.5 mg/L of aqueous MO solution under visible light for 4 hrs in the presence of different Al doped ZnO thin films spray-coated with 3 g of respective solutions

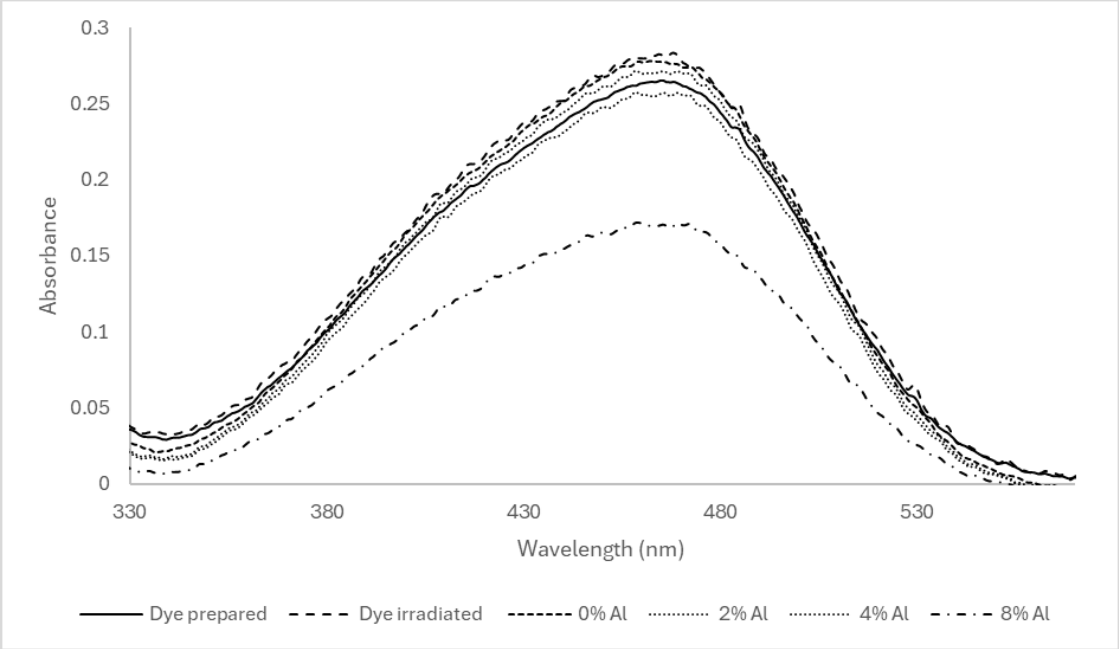

Figure 31. Absorbance spectra for the decomposition of 2.5 mg/L of aqueous MO solution under visible light for 4 hrs in the presence of different Al doped ZnO thin films spray-coated with 6 g of respective solutions

Figures 30 and 31 above illustrate the degradation of MO dye under visible light by the fabricated Al-doped ZnO thin films. The decrease in the absorbance intensity and shift of absorbance peak position were regarded as degradation of the methyl orange dye [137]. The thin films spray-coated with 3 grams of corresponding solutions showed the best degradation in contrast with the one spray-coated with 6 grams. This could be due to the porosity of the thin films resulting from less spray-coating solution used, allowing more adsorption and contact between the thin film and the dye pollutant. When thin films are deposited on a substrate, there is less contact with the pollutant molecules, especially the most crystalline ones, and this may reduce the photocatalytic reaction [18]. The XRD results showed that the Al-doped ZnO thin films spray-coated with 3 grams of solutions are less crystalline than the ones spray-coated with 6 grams of solution, and this may be another factor contributing to the

difference in their photocatalytic activities. The degradation increased with an increase in the doping mole% of the Al-doped ZnO thin films used. The highest degradation was attained for 8% Al-doped ZnO thin films for both thin films spray-coated with 3 and 6 grams of corresponding solutions. The enhancement of the photocatalytic degradation of Al-doped ZnO thin films can also be linked to the many electron traps introduced by Al^{3+} ions, as doping with Al^{3+} ions creates electron-trapping centres in the thin films, where electrons can be trapped and are prevented from recombining with the holes in the valence band [18, 133]. This leads to the longer lifetime of electrons, which enhances the production of hydroxyl and superoxide radicals and enhances the photocatalytic reaction [18, 133]. In comparison to other studies, the MO degradation rates of Al-doped ZnO thin films, unlike Ni-doped ZnO thin films, are good, considering the reaction conditions used, such as only a power of 10 W, no continuous stirring during irradiation time, no adjustment to solution pH or temperatures, and many other parameters explored in the literature for optimum results [18, 19, 36]. Since a degradation of MO was successful in the presence of Al-doped ZnO thin films under visible light, the possibility of being degraded under UV light is high because UV light has high energy wavelengths in comparison to visible light. These results also prove that aluminium is a good dopant for doping into ZnO to improve the photoresponse action of ZnO thin films.

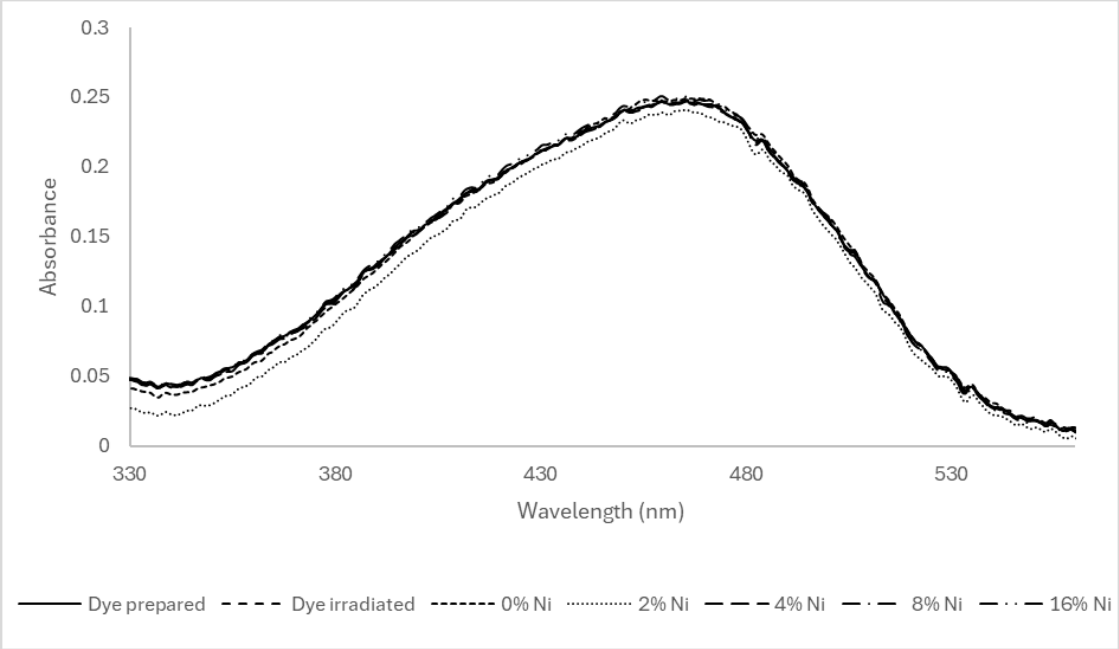

Figure 32. Absorbance spectra for the decomposition of 2.5 mg/L of aqueous MO solution under visible light for 4 hrs in the presence of different Ni doped ZnO thin films spray-coated with 3 g of respective solutions

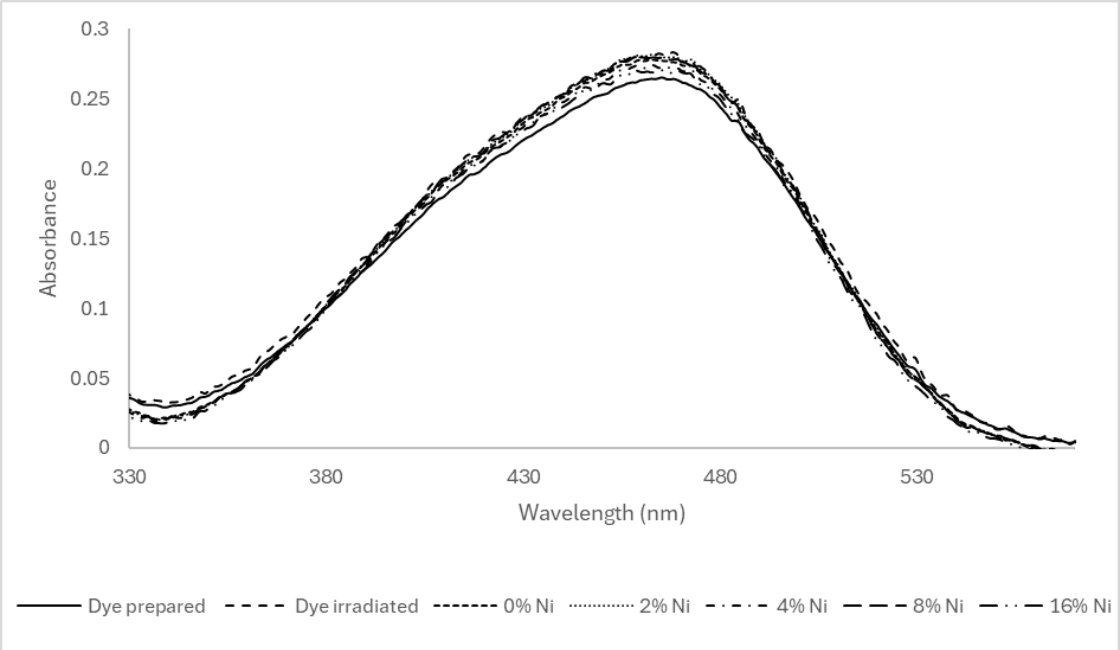

Figure 33. Absorbance spectra for the decomposition of 2.5 mg/L of aqueous MO solution under visible light for 4 hrs in the presence of different Ni doped ZnO thin films spray-coated with 6 g of respective solutions

As shown in figures 32 and 33 above, a very slight to no degradation was observed for the degradation of MO in the presence of Ni-doped ZnO thin films. The only MO dye degradation in the presence of Ni-doped ZnO thin films was attained for the 2% Ni-doped ZnO thin film spray-coated with 3 grams of the corresponding solution. The same results were attained in reference [138], where doping of over five percent Ni metal ions into ZnO thin films extremely narrowed the bandgap, and since the bandgap was narrow, the electrons moved back and forth easily between the valence and conduction band, which resulted in negligible photocatalytic activity. Doping ZnO with Ni creates a new bandgap level, where the bandgap is either increased or decreased [133]. With the slight degradation obtained for the 2% Ni-doped ZnO thin film, it may be that the bandgap narrowed with an increase in doping percentages, resulting in increased electron-hole recombination. This is because at 2% Ni-doped ZnO thin film spray-coated with 3 grams, there is less metal content in comparison to the 2% Ni-doped ZnO thin film spray-coated with 6 grams; thus, a slight degradation is obtained, but with double the metal contents deposited unevenly and being more crystalline, no degradation is observed. And at percentages higher than 2%, the bandgap may have decreased rapidly, leading to increased electron-hole recombination and no photocatalytic activities. Some of the photodegradation results depict an increase in the dye concentration in the presence of Ni-doped ZnO thin films, which may be because the dye was partially degraded, as the methyl orange dye was described to be a strongly bonded dye that is not easy to break down, and stronger forces are needed to induce its degradation [136]. The dye forms seven intermediates before its final degradation into a harmless product [136]. It was reported that the accumulation of intermediates on the surface of the photocatalyst blocks the active site and reduces light absorption, which ultimately leads to a decreased photocatalytic

reaction rate [23]. On the other hand, the parameters used, specifically the power, may not be sufficient to successfully degrade MO dye in the presence of Ni-doped ZnO thin films due to insufficient excitation of electrons. Stronger light intensity can excite more electron-hole pairs fast, and this speeds up the photodegradation [139]. The duration of irradiation may be short for complete degradation of intermediates. In another study, a lengthy irradiation time was required for absolute degradation of the dye with a low concentration while using a doped ZnO thin film photocatalyst [18]. The generation of recombination sites and the blocked surfaces of the photocatalysts may also be the cause of the decreased photocatalytic activity of Ni-doped ZnO thin films [133]. In a study where the photocatalytic activities of both Al- and Ni-doped ZnO thin films were studied, the same results as for this study were obtained [133]. The study points out that the improved photocatalytic activity of the Al-doped ZnO photocatalyst is due to the high surface area, the improvement of the absorption of light, and the increase of free charge carriers introduced by Al^{3+} ions. Whereas the decreased photocatalytic activity of the Ni-doped ZnO photocatalyst is attributed to the creation of recombination centres in the band gap and/or the reduction of active sites present on the surface [133]. All in all, it can be concluded that increased absorption of light does not always mean an increase in photocatalytic activity, and this can simply be because the light used during optical characterisation is different from the one used during the photocatalytic process [133, 140].

4.5. Degradation efficiency

By using formula 4 below, the percentage degradation (% D) efficiency was determined. Firstly, the molar absorption coefficient (ϵ) was calculated using equation

2 derived from the Beer Lambert Law. The absorbance measurements were all taken at a wavelength of 464 nm, which corresponds to the absorbance wavelength of methyl orange in UV-Vis spectroscopy as stated in [136].

Beer Lambert Law: $A = \varepsilon cl$.....1

$\varepsilon = A/cl$..… ……...…….....….2

In the equations above, A is the absorbance of light, c is the concentration of the dye solution in mol L^{-1}, l is the length of the solution the light passes through in cm, and ϵ is the molar absorption coefficient having the unit L mol^{-1} cm^{-1}. Prior to calculating the percentage degradation efficiency, the concentrations of the MO dyes were calculated using equation 3 derived from the Beer Lambert Law.

$C = A/\varepsilon l$..…….....….3

Dye degradation efficiency: $\% D = (C_o - C_t) / C_o \times 100$……..4

In equation 4 above, C_0 denotes the initial dye concentration, and C_t represents the dye concentration after irradiation time (hours). Table 3 below shows the concentration values of the MO solution before and after 4 hours of irradiation with visible light.

Table 3. Concentration values of methyl orange dye before and after irradiation with visible light in the presence of Al and Ni-doped ZnO thin films

Type of thin film used	**Initial concentration (in mg/L)**	**Final concentration (in mg/L)**	**Final concentration (in mg/L)**
		3 g thin film	**6 g thin film**

Dye irradiated **w/o** photocatalyst	2.5	2.5	2.5
Undoped ZnO	2.5	2.5	2.6
2% Al-doped ZnO	2.5	2.0	2.6
4% Al-doped ZnO	2.5	1.3	2.4
8% Al-doped ZnO	2.5	1.2	1.6
2% Ni-doped ZnO	2.5	2.4	2.7
4% Ni-doped ZnO	2.5	2.5	2.6
8% Ni-doped ZnO	2.5	2.5	2.6
16% Ni-doped ZnO	2.5	2.5	2.6

Table 3 above shows the concentration of the methyl orange solutions before and after irradiation with visible light. The concentration of methyl orange solution remained the same after 4 hours of visible light irradiation when the photocatalyst was not used. This is proof of the steadiness of the MO dye during photocatalysis experiments. Nonetheless, in the presence of the various thin film photocatalysts, a change in concentration of the MO dye was observed. The uncertainty encountered in the dye absorbance measurements was that the dye absorbance measurements were influenced by the noise in the laboratory, arising in slightly irregular absorbance curves and which led to the need to re-read the solutions multiple times.

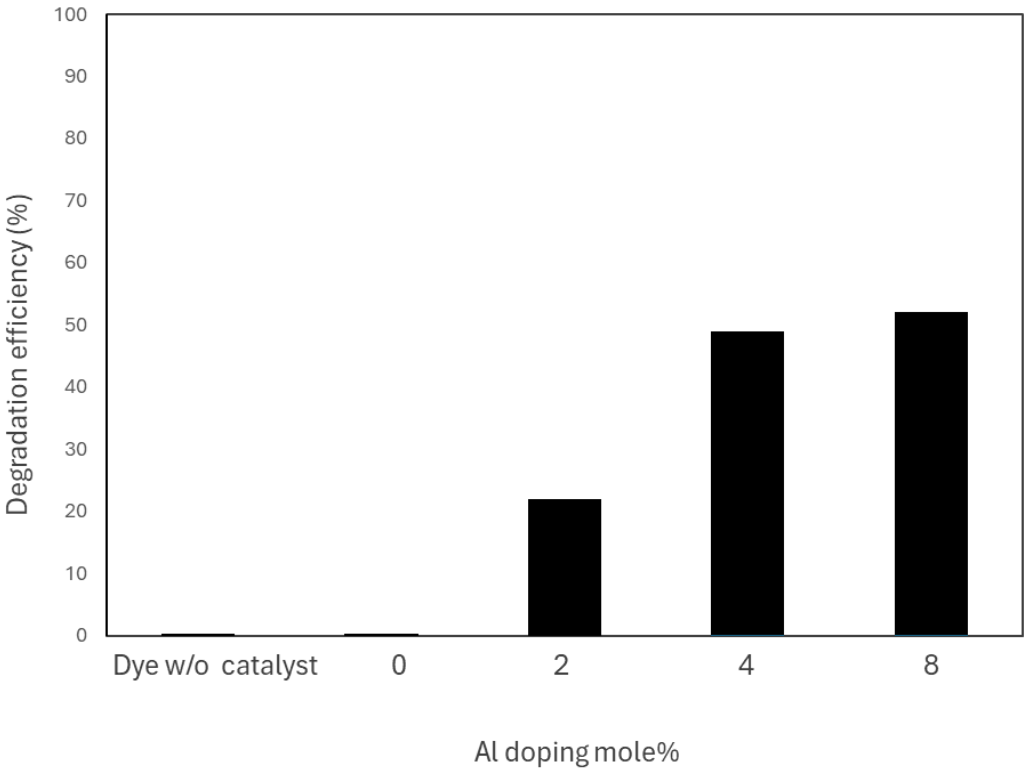

Figure 34. Degradation efficiency of methyl orange in the presence of Al-doped ZnO thin films spray-coated with 3 g of the corresponding solutions for the desired thin films

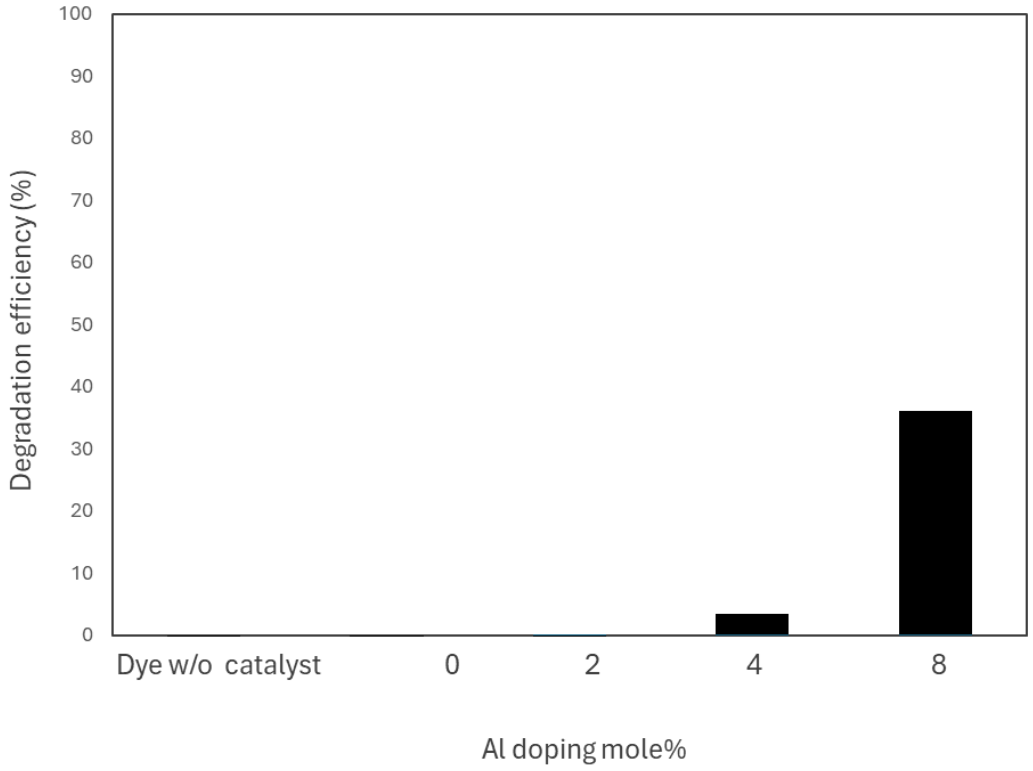

Figure 35. Degradation efficiency of methyl orange in the presence of Al-doped ZnO thin films spray-coated with 6 g of the corresponding solutions for the desired thin films

In the bar graphs above, the degradation efficiencies of MO in the presence of Al-doped ZnO thin films spray-coated with 3 and 6 grams of solutions are shown. The highest degradation efficiency of 52% was obtained for 8% Al-doped ZnO thin film spray-coated with 3 grams of corresponding solution. The difference between the degradation efficiency in the presence of 4 and 8% Al-doped ZnO thin films spray-coated with 3 grams of solution is quite minimal, but this was not observed for the thin films spray-coated with 6 grams of solution. Overall, Al-doped ZnO thin films spray-coated with 3 grams show the best degradation efficiency in contrast to the ones spray-coated with 6 grams. By comparison with that of undoped ZnO thin films, the degradation efficiency does increase by doping ZnO thin films with Al. It was

observed that the photocatalytic degradation efficiency follows the order AZO + MO > undoped ZnO + MO > MO.

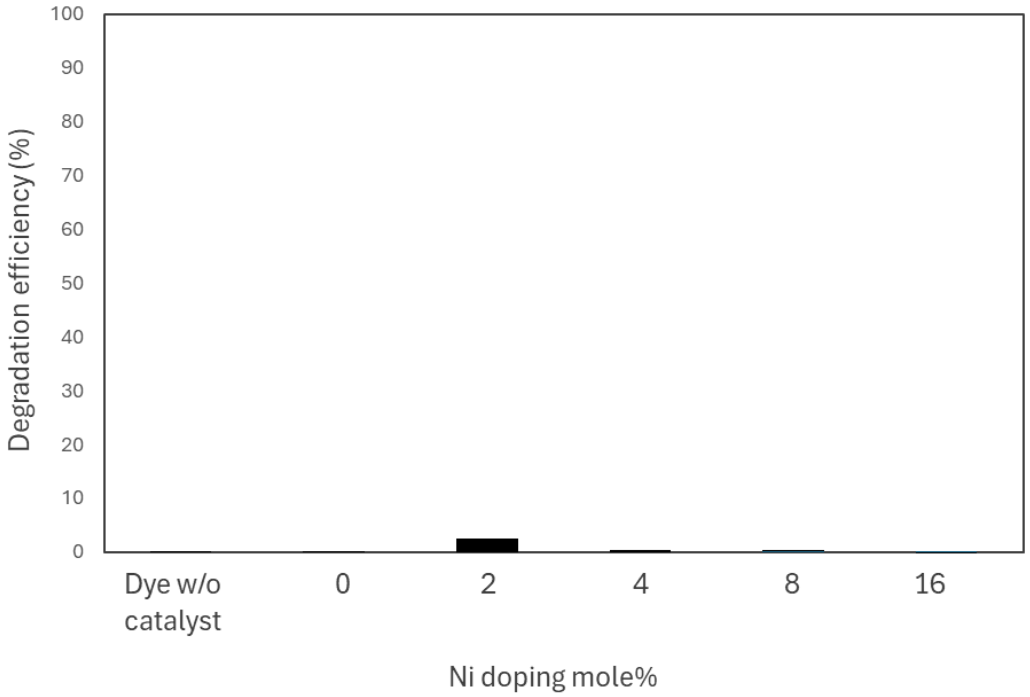

Figure 36. Degradation efficiency of methyl orange in the presence of Ni-doped ZnO thin films spray-coated with 3 g of the corresponding solutions for the desired thin films

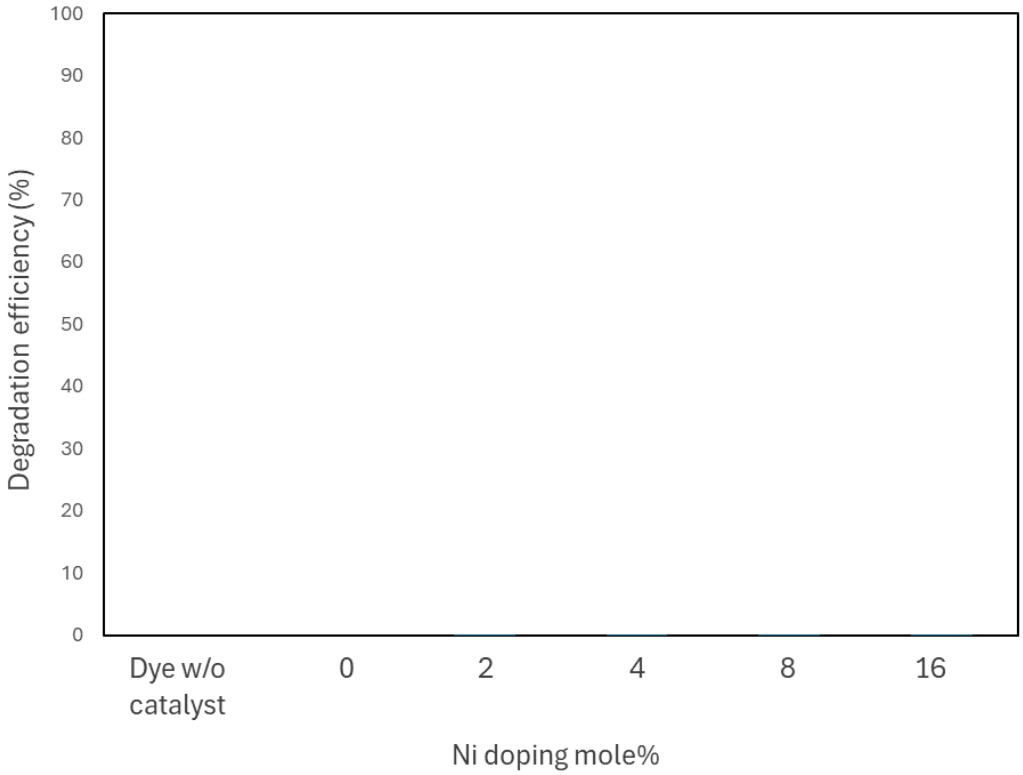

Figure 37. Degradation efficiency of methyl orange in the presence of Ni-doped ZnO thin films spray-coated with 6 g of the corresponding solutions for the desired thin films

The bar graphs above show the degradation efficiency of MO by Ni-doped ZnO thin films. The only degradation efficiency of 2.5% was attained when a 2% Ni-doped ZnO thin film spray-coated with 3 grams of solution was used. The same results were reported, where only the 1% Ni-doped ZnO thin films gave the best photodegradation efficiency [138]. In the present study, the degradation efficiency for both thin films spray-coated with 3 and 6 grams does not have a trend. The degradation efficiency of thin films spray-coated with 3 grams was shown to be around 0.26% except for 2% Ni-doped ZnO thin film. The degradation efficiency of thin films spray-coated with 6 grams was observed to be null. These results indicate that the Ni-doped ZnO thin films do not have the best photocatalytic activity under the degradation conditions used in

this study. Although there are studies that have documented successful photodegradation in the presence of Ni-doped ZnO thin films [19, 36, 133], the conditions (power, pH, concentration, temperatures) were varied to attain the best results.

These results will aid in fabricating the best thin films for various industrial applications; for instance, the thin films fabricated with 3 grams of precursor solution were confirmed by XRD results to be less crystalline than the ones fabricated with 6 grams of the precursor solutions. This means that the ones fabricated with 3 grams of precursor solutions may be best for photocatalytic activities, while the one spray-coated with 6 grams of solutions may be best for protective coatings and photovoltaic devices fabrication. The ammonium aluminium oxalate synthesised in this study opens pathways for its synthesis for research and industrial applications. The results on the ammonium aluminium oxalate solubility allow for future studies to optimise synthesis conditions to enhance purity and structural stability, which is vital for precursor solutions preparation for thin films fabrication. The UV-Vis results having highlighted the various factors affecting the absorption and transmittance of light in thin films will help future researchers to advance factors such as thin film thickness, heat treating temperature and even distribution of precursor solutions when fabricating thin films for various uses. The photocatalytic results of this research may be useful for industrial applications in the production of hydrogen via water splitting.

CHAPTER 5: CONCLUSION

All in all, the objectives of the study were achieved, which were to prepare the precursor solutions containing the respective metal ions, fabricate thin films through the aqueous spray-coating method, and characterise them using the XRD, UV-Vis spectrophotometer, and SEM, and finally, to investigate their photocatalytic activities. In this research, ammonium aluminium oxalate salt was successfully synthesised, confirmed by FTIR analysis. The XRD results showed that the thin films fabricated exhibit an intense peak at the (002) plane indicative of the stable hexagonal wurtzite phase of ZnO. The doping of ZnO with Al led to decreased peak intensity and broadening in the XRD patterns, indicating changes in the ZnO crystal structure. Similarly, Ni doping caused a reduction in peak intensities, confirming structural alterations. These changes altogether demonstrate the successful incorporation of Al and Ni dopants into the ZnO lattice. All the fabricated thin films showed an absorbance of light in the visible region of the electromagnetic spectrum. The photocatalytic activities of the fabricated thin films were evaluated by degradation of the methyl orange dye under visible light. It was concluded that the 8% Al-doped ZnO thin films fabricated in this study have good photocatalytic activity, likely due to increased electron-accepting centres and reduced electron-hole recombination. The good photocatalytic activities of 8% Al-doped ZnO thin films implicate their potential for improving PEC water splitting. The 8% Al-doped ZnO thin films fabricated in this study may be used as photoanodes for hydrogen production via PEC water splitting, this is because the process of photocatalysis is identical to that of water splitting. The successful use of Al-doped ZnO thin films contributes to the development of cost-effective and scalable materials for the production of clean energy. The Ni-doped ZnO thin films fabricated in this research exhibited poor photocatalytic activities, which

may be due to the presence of recombination centres or insufficient light power. The effects of the spray-coating solutions used to fabricate thin films were observed firstly in the colour of the thin films fabricated, the difference in the XRD patterns, and the absorbance of light, as well as the photocatalytic activities of the thin films. These results demonstrate that various dopants result in different properties of thin films; in this case, the optical (absorbance and transmittance), structural, and photocatalytic properties. While the study objectives were achieved successfully, challenges and limitations such as precursor solutions insolubility and instability at higher doping mole percentages and poor thin film adhesion to the supporting substrate at higher doping mole percentages were encountered. Specifically, for the preparation of precursor solutions for fabricating Al-doped ZnO thin films, insoluble precipitates formed for percentages higher than 8%, hence the study ended at 8% Al-doped ZnO thin films. On the other hand, poor thin film adhesion was experienced with the fabrication of higher than 16 % Ni-doped ZnO thin films. Ultimately, this investigation contributes to the development of a simple yet effective method for the fabrication of Al- and Ni-doped ZnO thin films, which is the aqueous spray-coating method.

CHAPTER 6: RECOMMENDATIONS

For this research, the author strongly recommends characterising the thin films after their fabrication using the necessary instruments available to verify the accuracy of the fabrication process and to facilitate the analysis and interpretation of the results before proceeding further. The focus on finding alternative Al^{3+} salts to obtain a clear and homogeneous coating solution even at higher doping concentrations is recommended, as the photocatalytic activities of Al-doped ZnO thin films were observed to improve with an increase in Al doping amount. The characterisation of all the fabricated thin films with SEM is highly recommended for better understanding and interpretation of results. It is also suggested to look into the long-term stability and durability of the thin films under prolonged visible light irradiation and in aqueous environments to ensure their feasibility for PEC water-splitting and other photocatalytic applications. The optimisation of the spray-coating method, including parameters such as spray time, substrate temperature, and deposition rate, may improve the consistency and quality of the films, especially at higher doping concentrations. Further studies that can be done on this research are the degradation of methyl orange using higher visible light power and investigating the applications of the fabricated thin films with good photocatalytic activities as photoanodes for hydrogen production via photoelectrochemical water splitting.

CHAPTER 7: REFERENCES

[1] Luo H, Zeng Z, Zeng G, et al. Recent progress on metal-organic frameworks based- and derived- photocatalysts for water splitting. *Chem Eng J* 2020; 383: 123196.

[2] Khan HR, Akram B, Aamir M, et al. Fabrication of Ni^{2+} incorporated ZnO photoanode for efficient overall water splitting. *Appl Surf Sci* 2019; 490: 302–308.

[3] Cai J, Ding J, Wei D, et al. Coupling of Ru and O-Vacancy on 2D Mo-Based Electrocatalyst Via a Solid-Phase Interface Reaction Strategy for Hydrogen Evolution Reaction. *Adv Energy Mater*; 11. Epub ahead of print 2021. DOI: 10.1002/aenm.202100141.

[4] Hausmann JN, Schlögl R, Menezes PW, et al. Is direct seawater splitting economically meaningful? *Energy Environ Sci* 2021; 14: 3679–3685.

[5] Park JH, Kim H. Zinc Oxide Nanostructured Thin Film as an Efficient Photoanode for Photoelectrochemical Water Oxidation. *Korean J Mater Res* 2020; 30: 441–446.

[6] Lewis NS, Nocera DG. Powering the planet: Chemical challenges in solar energy utilization. *Proc Natl Acad Sci U S A* 2016; 103: 15729–15735.

[7] Yumin H, Thomas H DW. Thin Film Photoelectrodes for Solar Water Splitting. *Chem Soc Rev Manuscr*; 2019-Novem. Epub ahead of print 2019. DOI: 10.1039/x0xx00000x.

[8] Realpe A, Núñez D, Carbal I, et al. Preparation and characterization of titanium dioxide photoelectrodes for generation of hydrogen by

photoelectrochemical water splitting. *Int J Eng Technol* 2015; 7: 753–759.

[9] Brinkert K. *Biomimetic systems for artificial photosynthesis*. 2018. Epub ahead of print 2018. DOI: 10.1007/978-3-319-77980-5_8.

[10] Kawawaki T, Mori Y, Wakamatsu K, et al. Controlled colloidal metal nanoparticles and nanoclusters : recent applications as cocatalysts for improving photocatalytic water-splitting activity. 2020; 16081–16113.

[11] Bellani S, Antognazza MR, Bonaccorso F, et al. Carbon-Based Photocathode Materials for Solar Hydrogen Production. *Adv Mater* 2019; 31: 1–95.

[12] Jiang C, Moniz SJA, Wang A, et al. Photoelectrochemical devices for solar water splitting – materials and challenges. 2017; 46: 4645–4660.

[13] Glasscock JA, Barnes PRF, Plumb IC, et al. Enhancement of photoelectrochemical hydrogen production from hematite thin films by the introduction of Ti and Si. *J Phys Chem C* 2007; 111: 16477–16488.

[14] Fernandez-Ibanez P, McMichael S, Rioja Cabanillas A, et al. New trends on photoelectrocatalysis (PEC): nanomaterials, wastewater treatment and hydrogen generation. *Curr Opin Chem Eng*; 34. Epub ahead of print 2021. DOI: 10.1016/j.coche.2021.100725.

[15] Khan HR, Akram B, Aamir M, et al. Electronic Tuning of Zinc Oxide by Direct Fabrication of Chromium (Cr) incorporated photoanodes for Visible-light driven Water Splitting Applications. *Sci Rep* 2020; 10: 1–10.

[16] Saoud T, Benramache S, Diha A. THE EFFECT OF Co AND Cu CO-DOPING ZnO THIN FILMS ON STRUCTURAL AND OPTICAL PROPERTIES. *Chem Didact Ecol Metrol* 2023; 28: 171–178.

[17] Khan HR, Aamir M, Akram B, et al. Superior visible-light assisted water splitting performance by Fe incorporated ZnO photoanodes. *Mater Res Bull*; 122. Epub ahead of print 2020. DOI: 10.1016/j.materresbull.2019.110627.

[18] Islam MR, Rahman M, Farhad SFU, et al. Structural, optical and photocatalysis properties of sol–gel deposited Al-doped ZnO thin films. *Surfaces and Interfaces*; 16. Epub ahead of print 2019. DOI: 10.1016/j.surfin.2019.05.007.

[19] Sellam M, Azizi S, Bouras D, et al. Degradation of rhodamine B dye under visible and solar light on zinc oxide and nickel-doped zinc oxide thin films. *Opt Mater (Amst)* 2024; 151: 115316.

[20] White JL, Baruch MF, Pander JE, et al. Light-Driven Heterogeneous Reduction of Carbon Dioxide: Photocatalysts and Photoelectrodes. *Chem Rev* 2015; 115: 12888–12935.

[21] Sutanto H, Durri S, Wibowo S, et al. Rootlike Morphology of ZnO:Al Thin Film Deposited on Amorphous Glass Substrate by Sol-Gel Method. *Phys Res Int*; 2016. Epub ahead of print 2016. DOI: 10.1155/2016/4749587.

[22] Ilkhani M, Dejam L. Structural and optical properties of ZnO and Ni : ZnO thin films : the trace of post-annealing. *J Mater Sci Mater Electron* 2021; 32: 3460–3474.

[23] Boskabadi MR, Rogé V, Bazargan A, et al. An introduction to photocatalysis. In: Bazargan A (ed) *Photocatalytic Water and Wastewater Treatment*. London, 2022, pp. 2–3.

[24] Parihar NS, Saraswat SK. Photoelectrochemical water splitting: An ideal

technique for pure hydrogen production. *J Indian Chem Soc* 2020; 97: 1099–1103.

[25] Hishimone P. *The spray method for fabrication of functional thin films by designed molecular precursors in aqueous solutions*. Kogakuin University, 2019.

[26] RAO MC, SHEKHAWAT MS. a Brief Survey on Basic Properties of Thin Films for Device Application. *Int J Mod Phys Conf Ser* 2013; 22: 576–582.

[27] Acosta E. Thin Films/Properties and Applications. *Intech* 2021; i: 13.

[28] Khadher A, Farooqui M, Mohsin M, et al. Metal Oxide Thin Films: a Mini Review. *J Adv Sci Res* 2016; 7: 1–8.

[29] Nagai H, and Sato M. Molecular Precursor Method for Fabricating p-Type Cu_2O and Metallic Cu Thin Films. *Intech* 2017; i: 13.

[30] Wang Y, Li Z, Xiao J. Stretchable Thin Film Materials: Fabrication, Application, and Mechanics. *J Electron Packag Trans ASME* 2016; 138: 1–22.

[31] Hishimone PN, Nagai H, and Mitsunobu S. Methods of Fabricating Thin Films for Energy Materials and Devices. In: *Lithium-ion Batteries - Thin Film for Energy Materials and Devices*. IntechOpen, 2020. Epub ahead of print 8 July 2020. DOI: 10.5772/intechopen.85912.

[32] Lu L, Nagai H. *Lithium-ion Batteries - Thin Film for Energy Materials and Devices*. 2019. Epub ahead of print 2019. DOI: 10.5772/intechopen.73346.

[33] Chen Z, Dinh HN, Miller E. *Photoelectrochemical water splitting: standards, experimental methods, and protocols*. 2013. Epub ahead of print 2013. DOI: 10.1007/978-1-4614-8298-7.

[34] Manjunatha R, Usharani K, and Naik D. Synthesis and characterization of ZnO nanoparticles: A review. *Mater Today Proc* 2019; 8: 1095–1101.

[35] Ramadan S. *Deposition of zinc oxide transition metal doped and in polymer composites*. University of Manchester, https://pure.manchester.ac.uk/ws/portalfiles/portal/184634465/FULL_TEXT.PDF (2018).

[36] Al-mamun R, Iqbal Z, Rahim A. Enhanced photocatalytic activity of Cu and Ni-doped ZnO nanostructures : A comparative study of methyl orange dye degradation in aqueous solution. *Heliyon* 2023; 9: e16506.

[37] Johari S, Muhammad NY, Zakaria MR. Study of zinc oxide thin film characteristics. *EPJ Web Conf* 2017; 162: 1–4.

[38] Behera JK. *SYNTHESIS AND CHARACTERIZATION OF ZnO NANO-PARTICLES*. NATIONAL INSTITUTE OF TECHNOLOGY, ROURKELA, 2023. Epub ahead of print 2023. DOI: 10.1016/j.matpr.2023.01.389.

[39] Moezzi A, McDonagh AM, Cortie MB. Zinc oxide particles: Synthesis, properties and applications. *Chem Eng J* 2012; 185–186: 1–22.

[40] Pandiyarasan V, Shanmugapriya P, Thanuja M, et al. Synthesis and characterization of ZnO nanoparticles. *Mater Today Proc* 2014; 3: 94–101.

[41] Gartner M, Stroescu H, Mitrea D, et al. Various Applications of ZnO Thin Films Obtained by Chemical Routes in the Last Decade. *Molecules*; 28. Epub ahead of print 2023. DOI: 10.3390/molecules28124674.

[42] Wang J, Chen R, Xiang L, et al. Synthesis, properties and applications of ZnO nanomaterials with oxygen vacancies: A review. *Ceramics International*; 44.

Epub ahead of print 2018. DOI: 10.1016/j.ceramint.2018.02.013.

[43] Yoo H, Heo K, Ansari MHR, et al. Recent advances in electrical doping of 2d semiconductor materials: Methods, analyses and applications. *Nanomaterials*; 11. Epub ahead of print 2021. DOI: 10.3390/nano11040832.

[44] Sen P, Bhattacharya P, Mukherjee G, et al. Advancements in Doping Strategies for Enhanced Photocatalysts and Adsorbents in Environmental Remediation. *Technologies* 2023; 11: 1–31.

[45] Rakshit Ameta SCA. *Photocatalysis: Principles and Applications*, http://scioteca.caf.com/bitstream/handle/123456789/1091/RED2017-Eng-8ene.pdf?sequence=12&isAllowed=y%0Ahttp://dx.doi.org/10.1016/j.regsciurbeco.2008.06.005%0Ahttps://www.researchgate.net/publication/305320484_SISTEM_PEMBETUNGAN_TERPUSAT_STRATEGI_MELESTARI (2017).

[46] Ebrahimi R, Hossienzadeh K, Maleki A, et al. Effects of doping zinc oxide nanoparticles with transition metals (Ag, Cu, Mn) on photocatalytic degradation of Direct Blue 15 dye under UV and visible light irradiation. *J Environ Heal Sci Eng* 2019; 17: 479–492.

[47] Ola O, Maroto-Valer MM. Review of material design and reactor engineering on TiO_2 photocatalysis for CO2 reduction. *J Photochem Photobiol C Photochem Rev* 2015; 24: 16–42.

[48] Hassaan MA, El MA, Marwa N. *Principles of Photocatalysts and Their Different Applications : A Review*. Springer International Publishing. Epub ahead of print 2023. DOI: 10.1007/s41061-023-00444-7.

[49] Kumar N, Srivastava A. Enhancement in UV emission and band gap by Fe

doping in ZnO thin films. *Opto-Electronics Rev* 2018; 26: 1–10.

[50] Chakrabortty T, Mina S, Habib A, et al. Fabrication and Characterization of Al Doped ZnO Thin Film Using Spin Coating Deposition System. 2018; 10: 70–76.

[51] Wang J, Shen W, Zhang X, et al. Preparation and characterization of (Al, fe) codoped zno films prepared by sol–gel. *Coatings*; 11. Epub ahead of print 2021. DOI: 10.3390/coatings11080946.

[52] Ramírez AE, Montero-Muñoz M, López LL, et al. Significantly enhancement of sunlight photocatalytic performance of ZnO by doping with transition metal oxides. *Sci Rep*; 11. Epub ahead of print 1 December 2021. DOI: 10.1038/s41598-020-78568-9.

[53] Iqbal A, Mahmood A, Muhammad T, et al. Structural and optical properties of Cr doped ZnO crystalline thin films deposited by reactive electron beam evaporation technique. *Prog Nat Sci Mater Int* 2013; 23: 64–69.

[54] Zaouchea C, Dahbib L, Benramachea S, et al. Study the effect of Ni doping on structural, optical and electrical properties of $Zn1\text{-}_xNi_xO$ thin films deposited by spray pyrolysis technique. *J Ovonic Res* 2023; 19: 197–205.

[55] Pati S. THIN FILM GROWTH TECHNIQUES : IMPORTANCE OF THIN FILMS Sumati Pati. *Int J Adv Technol Eng Sci* 2015; 3: 163–168.

[56] Sanjeev S, Kekuda D. Effect of annealing temperature on the structural and optical properties of zinc oxide (ZnO) thin films prepared by spin coating process. *IOP Conf Ser Mater Sci Eng*; 73. Epub ahead of print 2015. DOI: 10.1088/1757-899X/73/1/012149.

[57] Srinatha N, Raghu P, Mahesh HM, et al. Spin-coated Al-doped ZnO thin films for optical applications: Structural, micro-structural, optical and luminescence studies. *J Alloys Compd* 2017; 722: 888–895.

[58] Grosso D. How to exploit the full potential of the dip-coating process to better control film formation. *J Mater Chem* 2011; 21: 17033–17038.

[59] Yi SH, Kim JY, Jung WG. Properties of aluminum doped zinc oxide thin film prepared by sol-gel process. *Korean J Mater Res* 2010; 20: 351–355.

[60] Ambedkar AK, Singh M, Kumar V, et al. Structural, optical and thermoelectric properties of Al-doped ZnO thin films prepared by spray pyrolysis. *Surfaces and Interfaces* 2020; 19: 100504.

[61] Min YS, An CJ, Kim SK, et al. Growth and characterization of conducting ZnO thin films by atomic layer deposition. *Bull Korean Chem Soc* 2010; 31: 2503–2508.

[62] Yaghoubi S, Mousavi SM, Babapoor A, et al. Photocatalysts for solar energy conversion: Recent advances and environmental applications. *Renew Sustain Energy Rev* 2024; 200: 114538.

[63] Sun L, Yuan G, Gao L, et al. Chemical vapour deposition. *Nat Rev Methods Prim*; 1. Epub ahead of print 2021. DOI: 10.1038/s43586-020-00005-y.

[64] Hamedani Y, Macha P, Bunning TJ, et al. Plasma-Enhanced Chemical Vapor Deposition: Where we are and the Outlook for the Future. *Intech* 2016; 11: 13.

[65] Ahmadi S, Asim N, Alghoul MA, et al. Research and Development Aspects on Chemical Preparation Techniques of Photoanodes for Dye Sensitized Solar Cells. *Int J Photoenergy* 2014; 2014: 21.

[66] Marin E, Lanzutti A, Andreatta F, et al. Atomic layer deposition: State-of-the-art and research/industrial perspectives. *Corros Rev* 2011; 29: 191–208.

[67] Johnson RW, Hultqvist A, Bent SF. A brief review of atomic layer deposition: From fundamentals to applications. *Mater Today* 2014; 17: 236–246.

[68] Praveen P. A Study of Established Methods of Thin Films for Fabrication with Energy Materials. 2018; 1700–1705.

[69] Antonio Arce-Plaza, Fernando Sánchez-Rodriguez, Maykel Courel-Piedrahita, Osvaldo Vigil Galán VH-C, López SR-V and MO, Caswell JM, et al. CdTe Thin Films: Deposition Techniques and Applications. *Intech* 2018; 11: 13.

[70] Soonmin H, Vanalakar SA, Galal A, et al. A review of nanostructured thin films for gas sensing and corrosion protection. 2019; 7: 433–451.

[71] Ogugua SN, Ntwaeaborwa OM, Swart HC. Latest development on pulsed laser deposited thin films for advanced luminescence applications. *Coatings* 2020; 10: 1–22.

[72] Chaudhari MN. Thin film Deposition Methods: A Critical Review. *Int J Res Appl Sci Eng Technol* 2021; 9: 5215–5232.

[73] Satya Sopan Mahato, Disha Mahata SP and SM. Sol-Gel Science and Technology in Context of Nanomaterials – Recent Advances. Epub ahead of print 2020. DOI: http://dx.doi.org/10.5772/intechopen.111378 Sol-gel.

[74] Shamsi MS, Ahmadi M, Sabet M. Al doped ZnO thin films; preparation and characterization. *J Nanostructures* 2018; 8: 404–407.

[75] MODAN EM, PLĂIAȘU AG. Advantages and Disadvantages of Chemical Methods in the Elaboration of Nanomaterials. *Ann "Dunarea Jos" Univ*

Galati Fascicle IX, Metall Mater Sci 2020; 43: 53–60.

[76] Bokov D, Turki Jalil A, Chupradit S, et al. Nanomaterial by Sol-Gel Method: Synthesis and Application. *Advances in Materials Science and Engineering*; 2021. Epub ahead of print 2021. DOI: 10.1155/2021/5102014.

[77] Singh VK. THIN FILM DEPOSITION BY SPRAY PYROLYSIS TECHNIQUES. 2017; 4: 910–918.

[78] Saleh AM, Dawood MO, Chiad SS, et al. Investigation physical properties of sprayed Cr doped ZnO thin films. *J Ovonic Res* 2023; 19: 663–672.

[79] Tyona MD. A theoritical study on spin coating technique. *Adv Mater Res* 2013; 2: 195–208.

[80] Mustafa HAM, Jameel DA. Modeling and the main stages of spin coating process: A review. *J Appl Sci Technol Trends* 2021; 2: 119–123.

[81] Yin Y. Advances and perspectives of spin coating techniques. *Appl Comput Eng* 2023; 7: 291–301.

[82] Butt MA. Thin-Film Coating Methods: A Successful Marriage of High-Quality and Cost-Effectiveness—A Brief Exploration. *Coatings*; 12. Epub ahead of print 2022. DOI: 10.3390/coatings12081115.

[83] Abdellah A, Baierl D, Fabel B, et al. Spray-coating deposition for large area organic thin-film devices. *Tech Proc 2009 NSTI Nanotechnol Conf Expo, NSTI-Nanotech 2009* 2009; 2: 447–450.

[84] Girotto C, Rand BP, Genoe J, et al. Exploring spray coating as a deposition technique for the fabrication of solution-processed solar cells. *Sol Energy Mater Sol Cells*; 93. Epub ahead of print 2009. DOI:

10.1016/j.solmat.2008.11.052.

[85] Tomulescu AG, Stancu V, Beşleagă C, et al. Reticulated Mesoporous TiO_2 Scaffold, Fabricated by Spray Coating, for Large-Area Perovskite Solar Cells. *Energy Technol*; 8. Epub ahead of print 2020. DOI: 10.1002/ente.201900922.

[86] Eslamian M. Spray-on thin film PV solar cells: Advances, potentials and challenges. *Coatings* 2014; 4: 60–84.

[87] Hishimone PN, Watarai K, Nagai H, et al. Thin film fabrication and characterization of layered rock salt $LiCoO_2$ on quartz glass spray-coated with an aqueous ammonia solution involving metal acetates. *Coatings* 2019; 9: 9–11.

[88] Hishimone P, Nagai H, Morita M, et al. Highly-Conductive and Well-Adhered Cu Thin Film Fabricated on Quartz Glass by Heat Treatment of a Precursor Film Obtained Via Spray-Coating of an Aqueous Solution Involving Cu(II) Complexes. *Coatings* 2018; 8: 352.

[89] Sukri MSNA, Shameli K, Isa MED, et al. Green Synthesis of Zinc Oxide-Based Nanomaterials for Photocatalytic Studies: A Mini Review. *IOP Conf Ser Mater Sci Eng* 2021; 1051: 012083.

[90] Maynez-navarro OD, Sanchez-salas J. Focus on Zinc Oxide as a Photocatalytic Material for Water Treatment. Epub ahead of print 2018. DOI: 10.29011/IJBB-106/100006.

[91] Kumari S, Sharma K, Korpal S, et al. A comprehensive study on photocatalysis: materials and applications. *CrystEngComm* 2024; 26: 4886–4915.

[92] Han J, Qiu W, Gao W. Potential dissolution and photo-dissolution of ZnO thin films. *J Hazard Mater* 2010; 178: 115–122.

[93] Nadareishvili M, Mamniashvili G, Jishiashvili D, et al. Investigation of the Visible Light-Sensitive ZnO Photocatalytic Thin Films. *Eng Technol Appl Sci Res* 2020; 10: 5524–5527.

[94] Kulis-Kapuscinska A, Kwoka M, Borysiewicz MA, et al. Photocatalytic degradation of methylene blue at nanostructured ZnO thin films. *Nanotechnology*; 34. Epub ahead of print 2023. DOI: 10.1088/1361-6528/aca910.

[95] Janani L, Henry K, Edwine K. Optimization of Photocatalytic Degradation of Reactive Blue Dye Using Zinc Oxide Catalyst. 2015; 2: 343–347.

[96] Park HW, Chung KB, Park JS, et al. Electronic structure of conducting Al-doped ZnO films as a function of Al doping concentration. *Ceram Int*; 41. Epub ahead of print 2015. DOI: 10.1016/j.ceramint.2014.09.102.

[97] Li L, Gao S, Zhang Z, et al. Effect of thermal shock on ZnO/Ag/ZnO nano-multilayers: Photoelectric property degradation. *Sol Energy*; 269. Epub ahead of print 2024. DOI: 10.1016/j.solener.2024.112331.

[98] Mohamadpour F, Amani AM. Photocatalytic systems: reactions, mechanism, and applications. *RSC Adv* 2024; 14: 20609–20645.

[99] Boskabadi MR, Rogé V, Bazargan A SH and BE. Photocatalytic Water and Wastewater Treatment. 2022.

[100] Malato S, Fernández-Ibáñez P, Maldonado MI, et al. Decontamination and disinfection of water by solar photocatalysis: Recent overview and trends.

Catal Today 2009; 147: 1–59.

[101] Mochane MJ, Motloung MT, Mokhena TC, et al. Morphology and Photocatalytic Activity of Zinc Oxide Reinforced Polymer Composites : A Mini Review. 12. Epub ahead of print 2022. DOI: https:// doi.org/10.3390/catal12111439.

[102] Li D, Kassymova M, Cai X, et al. Photocatalytic CO_2 reduction over metal-organic framework-based materials. 412.

[103] Wang Y, Wang S, Zhang SL, et al. Formation of Hierarchical $FeCoS_2$–CoS_2 Double-Shelled Nanotubes with Enhanced Performance for Photocatalytic Reduction of CO_2. *Angew Chemie - Int Ed* 2020; 59: 11918–11922.

[104] Han F, Kambala VSR, Srinivasan M, et al. Tailored titanium dioxide photocatalysts for the degradation of organic dyes in wastewater treatment: A review. *Appl Catal A Gen* 2009; 359: 25–40.

[105] Kansal SK, Kaur N, Singh S. Photocatalytic degradation of two commercial reactive dyes in aqueous phase using nanophotocatalysts. *Nanoscale Res Lett* 2009; 4: 709–716.

[106] Khan SA, Khan SB, Khan LU, et al. FTIR.pdf. *Handb Mater Charact* 2018; 317–344.

[107] Pasieczna-Patkowska S, Cichy M, Flieger J. Application of Fourier Transform Infrared (FTIR) Spectroscopy in Characterization of Green Synthesized Nanoparticles. *Molecules* 2025; 30: 1–36.

[108] Verma R. Introduction to Fourier Transform Infrared Spectrometry Introduction to FTIR, https://www.researchgate.net/publication/359706716

(2022).

[109] Ermrich M, Opper D. *X-ray Powder Diffraction for the Analyst*. 2011.

[110] Ali A, Chiang YW, Santos RM. X-Ray Diffraction Techniques for Mineral Characterization: A Review for Engineers of the Fundamentals, Applications, and Research Directions. *Minerals*; 12. Epub ahead of print 2022. DOI: 10.3390/min12020205.

[111] Lee HY. Synthesis of ammonium aluminum oxalate from Bayer aluminum hydroxide. *Mater Lett*; 65. Epub ahead of print 2011. DOI: 10.1016/j.matlet.2011.05.106.

[112] Azfar AK, Kasim MF, Lokman IM, et al. Comparative study on photocatalytic activity of transition metals (Ag and Ni)doped ZnO nanomaterials synthesized via sol–gel method. *R Soc Open Sci*; 7. Epub ahead of print 2020. DOI: 10.1098/rsos.191590.

[113] Nagai H, Sato M. Heat Treatment in Molecular Precursor Method for Fabricating Metal Oxide Thin Films. *Heat Treat - Conv Nov Appl*. Epub ahead of print 2012. DOI: 10.5772/50676.

[114] Muthuselvi C, Arunkumar A, Rajaperumal G. Growth and Characterization of Oxalic Acid Doped with Tryptophan Crystal for Antimicrobial Activity, www.pelagiaresearchlibrary.com (2017).

[115] Meshram SB, Kushwaha OS, Reddy PR, et al. Investigation on the effect of oxalic acid, succinic acid and aspartic acid on the gas hydrate formation kinetics. *Chinese J Chem Eng* 2019; 27: 2148–2156.

[116] Mary SS, Kirupavathy SS. An insight on spectral, microstructural, electrical

and mechanical characterization of ammonium oxalate monohydrate crystals. *Mater Sci Pol*. Epub ahead of print 2020. DOI: 10.2478/msp-2019-0087.

[117] Antonio M, Belderbos S, Yañez-vilar S, et al. Development of Superparamagnetic Nanoparticles Coated with Polyacrylic Acid and Aluminum Hydroxide as an Efficient Contrast Agent for Multimodal Imaging. 2019; 1–20.

[118] Pouran HM, Banwart SA, Romero-gonzalez M. Coating a polystyrene well-plate surface with synthetic hematite , goethite and aluminium hydroxide for cell mineral adhesion studies in a controlled environment. *Appl GEOCHEMISTRY* 2014; 42: 60–68.

[119] Ghazai AJ, Salman EA, Jabbar ZA. Effect of Aluminum Doping on Zinc Oxide Thin Film Properties Synthesis by Spin Coating Method. *Am Sci Res J Eng Technol Sci* 2016; 26: 202–211.

[120] Sandeep KM, Bhat S, Dharmaprakash SM. Nonlinear absorption properties of ZnO and Al doped ZnO thin films under continuous and pulsed modes of operations. *Opt Laser Technol*; 102. Epub ahead of print 2018. DOI: 10.1016/j.optlastec.2017.12.031.

[121] Karmakar R, Neogi SK, Banerjee A, et al. Structural; Morphological; optical and magnetic properties of Mn doped ferromagnetic ZnO thin film. *Appl Surf Sci*; 263. Epub ahead of print 2012. DOI: 10.1016/j.apsusc.2012.09.133.

[122] Das N, Majumdar R, Sen A, et al. Nanosized bismuth ferrite powder prepared through sonochemical and microemulsion techniques. *Mater Lett*; 61. Epub ahead of print 2007. DOI: 10.1016/j.matlet.2006.08.026.

[123] Vimalkumar T V., Poornima N, Kartha CS, et al. Effect of precursor medium on structural, electrical and optical properties of sprayed polycrystalline ZnO thin films. *Mater Sci Eng B*; 175. Epub ahead of print 2010. DOI: 10.1016/j.mseb.2010.06.012.

[124] Kumari N, Patel SR, Gohel J V. Optical and structural properties of ZnO thin films prepared by spray pyrolysis for enhanced efficiency perovskite solar cell application. *Opt Quantum Electron* 2018; 50: 1–22.

[125] Palanichamy S, Raj Mohamed J, Satheesh Kumar PS, et al. Volume of precursor solution effect on the properties of SnO2 thin films prepared by nebulized spray pyrolysis technique. *Opt Quantum Electron* 2018; 50: 1–19.

[126] Musaab Khudhr M, Abass KH. Effect of Al-Doping on the Optical Properties of ZnO Thin Film Prepared by Thermal Evaporation Technique. *Int J Eng Technol* 2016; 7: 25–31.

[127] Yasin Ahmed T, Aziz SB, M. A. Dannoun E. New photocatalytic materials based on alumina with reduced band gap: A DFT approach to study the band structure and optical properties. *Heliyon* 2024; 10: e27029.

[128] Mkawi EM, Ibrahim K, Ali MKM, et al. The effect of dopant concentration on properties of transparent conducting Al-doped ZnO thin films for efficient Cu_2ZnSnS_4 thin-film solar cells prepared by electrodeposition method. *Appl Nanosci* 2015; 5: 993–1001.

[129] Hur JS, Song J Bin, Kim J, et al. Efficiencies of CIGS solar cells using transparent conducting Al-doped ZnO window layers as a function of thickness. *J Korean Phys Soc* 2008; 53: 437–441.

[130] Agrohiya S, Dahiya S, Goyal PK, et al. Nickel Doped Zinc Oxide Thin Films for Visible Blind Ultraviolet Photodetection Applications. *ECS Sensors Plus* 2022; 1: 043601.

[131] Mathew JP, Varghese G, Mathew J. Structural and Optical Properties of Ni:ZnO Thin Films-Effect of Annealing and Doping Concentration. *SOP Trans Appl Phys* 2014; 1: 27–36.

[132] Ali MY, Khan MKR, Karim AMMT, et al. Effect of Ni doping on structure, morphology and opto-transport properties of spray pyrolised ZnO nano-fiber. *Heliyon* 2020; 6: e03588.

[133] Jellal I, Daoudi O, Nouneh K, et al. Comparative study on the properties of Al- and Ni-doped ZnO nanostructured thin films grown by SILAR technique : application to solar photocatalysis. *Opt Quantum Electron*; 55, https://doi.org/10.1007/s11082-023-04798-6 (2023).

[134] Ayachi M, Ayad F, Djelloul A, et al. Synthesis and Characterization of Ni-Doped ZnO Thin Films Prepared by Sol – Gel Spin-Coating Method. 2021; 55: 482–490.

[135] Owoeye VA, Ajenifuja E, Adeoye EA, et al. Microstructural and optical properties of Ni-doped ZnO thin films prepared by chemical spray pyrolysis technique. *Mater Res Express*; 6. Epub ahead of print 2019. DOI: 10.1088/2053-1591/ab26d9.

[136] Lau YY, Wong YS, Teng TT, et al. Degradation of cationic and anionic dyes in coagulation-flocculation process using bi-functionalized silica hybrid with aluminum-ferric as auxiliary agent. *RSC Adv* 2015; 5: 34206–34215.

[137] Shankar S, Saroja M, Venkatachalam M, et al. Photocatalytic degradation of methylene blue dye using ZnO thin films. 2017; 03: 180–188.

[138] Yin Q, Qiao R, Li Z, et al. Hierarchical nanostructures of nickel-doped zinc oxide: Morphology controlled synthesis and enhanced visible-light photocatalytic activity. *J Alloys Compd* 2015; 618: 318–325.

[139] Aghdam TR, Mehrizadeh H, Salari D, et al. Photocatalytic removal of NOx over immobilized $BiFeO_3$ nanoparticles and effect of operational parameters. *Korean J Chem Eng* 2018; 35: 994–999.

[140] Bakbolat B, Daulbayev C, Sultanov F, et al. Recent Developments of TiO_2-Based Photocatalysis in the Hydrogen Evolution and Photodegradation : A Review. *Nanomaterials* 2020; 10: 1–16.

5. CHAPTER 8: APPENDICES

Appendix A: Research ethical clearance certificate from UNAM

UNAM
UNIVERSITY OF NAMIBIA

ETHICAL CLEARANCE CERTIFICATE

Ethical Clearance Reference Number: SOS-0163 **Date: 23 AUGUST 2023**

This Ethical Clearance Certificate is issued by the University of Namibia Ethics Committee (REC) in accordance with the University of Namibia's Research Ethics Policy and Guidelines. Ethical approval is given in respect of undertakings contained in the Research Project outlined below. This Certificate is issued on the recommendations of the ethical evaluation done by the ethics committee.

Title of Project:	INVESTIGATIONS ON THE FABRICATION OF Al, Cr, AND Ni- DOPED ZNO THIN FILMS BY THE SPRAY-COATING METHOD AND THEIR APPLICATIONS AS PHOTOANODES FOR HYDROGEN PRODUCTION VIA PHOTOELECTROCHEMICAL WATER SPLITTING
Student:	WILKA TITUS
Student Number:	201703636
Supervisor(s):	Dr. PHILIPUS HISHIMONE

Centre for Research Services

Take note of the following:

1. Any significant changes in the conditions or undertakings outlined in the approved Proposal must be communicated to the ethics committee. An application to make amendments may be necessary.
2. Any breaches of ethical undertakings or practices that have an impact on ethical conduct of the research must be reported to the ethics committee.
3. The Principal Researcher must report issues of ethical compliance to the ethics committee (through the Chairperson) at the end of the Project or as may be requested by the ethics committee.
4. The ethics committee retains the right to:

i) Withdraw or amend this Ethical Clearance if any unethical practices (as outlined in the Research Ethics Policy) have been detected or suspected,
ii) Request for an ethical compliance report at any point during the course of the research.

The ethics committee wishes you the best in your research.

Dr. Zivayi Chiguvare (Chairperson Ethics Committee)

Prof. Davis Mumbengegwi (Head, Multidisciplinary Research)

Appendix B: Research permission letter from UNAM

CENTRE FOR RESEARCH SERVICES
Office of the Pro-Vice Chancellor: Research, Innovation & Development
University of Namibia, Private Bag 13301, Windhoek, Namibia
340 Mandume Ndemufayo Avenue, Pioneers Park, Office F223 - Block, Second Floor
☎ +264 61 206 4673; E-mail:smbulut@unam.na; URL: http://www.unam.edu.na

UNAM
UNIVERSITY OF NAMIBIA

RESEARCH PERMISSION LETTER

Date: 21/09/2023

Student Name: WILKA TITUS

Student Number: 201703636

Programme: MASTER OF SCIENCE IN CHEMISTRY

Approved Research Title: INVESTIGATIONS ON THE FABRICATION OF Al, Cr, AND Ni-DOPED ZNO THIN FILMS BY THE SPRAY-COATING METHOD AND THEIR APPLICATIONS AS PHOTOANODES FOR HYDROGEN PRODUCTION VIA PHOTOELECTROCHEMICAL WATER SPLITTING

TO WHOM IT MAY CONCERN:

I hereby confirm that the above-mentioned student is registered at the University of Namibia for the programme indicated. The proposed study met all the requirements as stipulated in the University guidelines and has been approved by the relevant committees.

The proposal adheres to ethical principles as per attached Ethical Clearance Certificate. Permission is hereby granted to carry out the research as described in the approved proposal.

Best Regards

Dr. AEE Shikongo
Head: Postgraduate Research Support Services
Tel: +264 61 206 3129
E-mail: aeshikongo@unam.na

CENTRE FOR RESEARCH SERVICES
Office of the Director
2023 -09- 21
University of Namibia
UNAM